Asia-Pacific GAW on Greenhouse Gases
Newsletter

Volume No.5
December, 2014

KMA Korea Meteorological Administration

GAW

Asia-Pacific GAW on Greenhouse Gases

Newsletter

Volume No.5
December, 2014

KMA Korea
Meteorological
Administration

GAW

KMA BMKG MANCHESTER 1824 N-IWA Taihoro Nukurangi KRISS 한국표준과학연구원 dongguk UNIVERSITY

The University of Manchester

Contents

Global atmosphere watch activities in Korea

Chulkyu Lee[*], Bok-Haeng Heo, Homan Lee, Yean-Hee Kim, Haeyoung Lee, Heejong Yoo, Sangsup Park, Jegyu Yu, Yungseok Yoo, Hyuk-Je Lee, Dong-Bong Yu, Taegyun Jeong, Han-Cheol Lim, Hongwoo Choi, Eunsil Kim, Seyoung Moon, Miyoung Ko

Korea Meteorological Administration (KMA) began the atmospheric composition watch in association with the Global Atmosphere Watch (GAW) Program of World Meteorological Organization (WMO) in 1987. Korea Global Atmosphere Watch Center (KGAWC), KMA is in charge of the GAW Program in Korea. Here we introduce the current status of the GAW related activities of KMA, in particular measurement stations, atmospheric measurement variables, and the GAW central facility such as World Calibration Centre (WCC) in Korea.

Measurement stations

KGAWC operates the measurement stations to collect and provide reliable scientific data and information on the chemical composition of the atmosphere, its natural and anthropogenic change, helping improve the understanding on climate change. There are the three main stations for the atmosphere watch, which are located in the west (at Anmyeon, Chungnam Province), south (at Gosan, Jeju), and east (at Ulleung, Gyungbook Province) of the Korean Peninsula, in aim of monitoring of transportation of the atmospheric substances and variation in the atmospheric composition over the Korean Peninsula.

KMA established a station for the atmosphere watch at Mt. Soback in the middle of South Korea in 1987, and then moved the station to Anmyeon in 1996. The Anmyeon (AMY) station was designated as a regional station in the Global Atmosphere Watch (GAW) program of World Meteorological Organization (WMO) in 1998. The Gosan (JGS) and Ulleung (ULL) stations began the atmosphere watch in 2009 and 2014, respectively. The

JGS station was designated as a GAW regional station in 2013. From the three stations, KMA collects the atmospheric observation data of 37 components in the fields of greenhouse gases, aerosols, reactive gases, stratospheric ozone, atmospheric radiation including ultraviolet (UV) radiation, and precipitation chemistry in the Korean Peninsula, in accordance with the measurement recommendations of the GAW program.[1] To collect more specific data, e.g. radioactivity (Radon), ozone sonde, vertical profiles of aerosol optical properties from LIDAR, and ultraviolet (UV), it designated universities, research institutes, or meteorological stations at Seoul, Pohang, Gwangju, Mokpo, Uljin, Gangneung, and Jeju as the auxiliary stations for the atmosphere watch.

In the AMY station (36.54 N, 126.33 E, 47 m above sea level), the abundances of carbon dioxide (CO_2), methane (CH_4), nitrous oxide (N_2O), chlorofluorocarbons (CFCs, CFC-11, 12,113), and sulfur hexafluoride (SF_6) are collected in the fields of greenhouse gases. The air sampled at the inlet on top of tower 40 m above ground level (47 m above sea level) goes to the instrument through decarbon tube for analysis, with high accuracy and precision, using cavity ring down spectroscopy (CRDS) for CO_2 and CH_4 at rate of 5 seconds and Gas Chromatography coupled with Electron Capture Detector (GC-ECD) for the others at rate of 1 hour. For SF_6 measurement, a preconcentrator using a thermal absorption and

Figure 1

Location of the atmospheric watch stations operated by KMA/KGAWC in the Korean Peninsula. Three main stations (yellow) located in the west, south, and east of the Korean Peninsula are operated by KMA. The eight auxiliary stations (white) designated by KMA are run by Seoul National University (SNU) and Yonsei University (YU) at Seoul, Gwangju Institute of Science and Technology (GIST) at Gwangju, Jeju University (JU) at Gosan, and KMA regional offices at Gangneung, Uljin, Pohang, and Mokpo. An auxiliary station in King Sejong Base in Antarctica is run by the Korea Polar Research Institute (KOPRI).

desorption method is adopted. Physical, chemical, and optical characteristics of aerosols, widely acknowledged as one of the most significant and uncertain aspects of climate change projections, have been measured with in-situ instruments, including their vertical profiles retrieved using a ground-based LIDAR. Ambient air for the aerosol measurements is sampled from the inlet on 10 m tower on the roof of the building, which meets the GAW aerosol sampling guideline.[2] In physical parameters, we collect atmospheric observation data of mass concentrations (PM1, PM2.5, PM10) with ß-ray absorption and/or laser scattering methods, and size distribution in the ranges of 0.01 − 0.5 µm with 54 chan-

nels (Scanning Mobility Particle Sizer), 0.5 – 20 μm with 52 channels (Aerodynamic Particle Sizer), and 0.25 – 32 μm with 31 channels (Grimm Dust Monitor) at the temporal resolution of 3 minutes. For the optical properties, it measures scattering and absorption coefficients by Nephelometer and Aethalometer, aerosol optical depth by sun-photometer at five wavelengths (368, 500, 675, 778, 862 nm) and precision filter radiometer at four wavelengths (368, 412, 500, 862 nm), vertical profiles of back-scattering coefficients, depolarization ratio, and color ratio from a LIDAR instrument with wavelengths of 1064 and 532 nm. The aerosols (TSP, PM2.5, PM10) were sampled for 24 hours once a week for analysis of the chemical components (F^-, Cl^-, NO_3^-, SO_4^{2-}, Na^+, NH_4^+, K^+, Mg^{2+}, Ca^{2+}) and metals (Al Ca, Fe, K, Mg, Na, S, Ti, Mn, Zn, Cu, V, Cr, Co, Ba, Pb, U). The reactive gases such as carbon monoxide (CO), surface ozone (O_3), nitrogen oxides (NO_x), and sulfur dioxide (SO_2) have been measured because the compounds play a role in the chemistry of the atmosphere and the formation of aerosols. It used instruments using gas-phase chemiluminescence for NO_x, UV fluorescence for SO_2, UV photometry for O_3, nondispersive infrared photometry for CO which is changing to CRDS for the maintenance. Regarding to the stratospheric ozone, total column ozone is measured using the Brewer spectrometers, together with UV and solar and terrestrial radiation. Precipitation chemistry observations focus on the acidity, conductivity, and major 9 ions (F^-, Cl^-, NO_3^-, SO_4^{2-}, Na^+, NH_4^+, K^+, Mg^{2+}, Ca^{2+}).

We have currently focused on greenhouse gases, reactive gases, aerosols, atmospheric radiation, stratospheric ozone, and precipitation chemistry at the Gosan (JGS) station (33.18 N, 126.12 E) and on the greenhouse gases, reactive gases, aerosols, atmospheric radiation, and precipitation chemistry at the Ulleung station (37.28 N, 130.53 E) (see Table 1 for the detailed information).

To maintain traceability and compatibility and secure the level of measurements, we have taken part in the inter-comparison campaigns under the auspices of Quality Assurance and Scientific Activity Centers (QA/SAC), in particular on greenhouse gases and precipitation chemistry. Recently we participated in the fifth round-robin comparison (RR5) in 2009 - 2012 organized by the WMO GAW Central Calibration Laboratory (CCL) in NOAA, and methane reference gas inter-comparisons organized by the World Calibration Center for CH_4 (WCC-CH_4) in Japan Meteorological Agency (JMA). We will also take part in the inter-comparison campaigns in 2015. In terms of precipitation chemistry, we participate in the GAW annual laboratory inter-comparison studies organized by World Data Centre for Precipitation Chemistry (WDCPC)

We also examine current and new methodologies for determination of baseline of greenhouse gas concentrations. New parameters and

Table 1. Atmospheric species related to the WMO GAW program, collected at three main stations (Anmyeon, Gosan, and Ulleung) and eight auxiliary stations managed by KMA and KMA-designated institutes in the Korean Peninsula

Site (Institute)	Greenhouse gases	Reactive gases	Aerosols	Stratospheric Ozone/UV	Atmospheric radiation	Precipitation Chemistry
Anmyeon (KMA)	CO_2, CH_4, N_2O, CFCs, SF_6	CO, NO_x, SO_2, O_3	Physical[1] Optical[2] Chemical[3]	TCO,[4] UV-A,B	Solar Terrestrial	Acidity Conductivity Ions[5]
Gosan (KMA)	CO_2, CH_4, N_2O,	CO, NO_x, SO_2, O_3	Physical[6] AOD	TCO, UV-A,B	Solar Terrestrial	Acidity Conductivity Ions
Ulleung (KMA)	CO_2, CH_4, N_2O, SF_6	CO	Physical[7] AOD	UV-A,B	Solar Terrestrial	Acidity Conductivity Ions
Pohang (KMA)				TCO, Profile[8] UV-A,B		
Mokpo (KMA)				UV-A,B		
Uljin (KMA)						Acidity Conductivity Ions
Gangneung (KMA)				UV-A,B		
Gosan (JU)		Radon				
Seoul (SNU)	CO_2, H_2O					
Seoul (YSU)				TCO, UV-A,B		
Gwangju (GIST)			Optical[9]			

1) $PM_{1,2.5,10}$, size distribution (0.01-32 μm), total suspended particle (TSP)
2) Scattering/absorption coefficients, aerosol optical depth (AOD), and vertical profiles of backscattering coefficient, depolarization ratio, and color ratios
3) Chemical ions (F^-, Cl^-, NO_3^-, SO_4^{2-}, Na^+, NH_4^+, K^+, Mg^{2+}, Ca^{2+}) and metals (Al Ca, Fe, K, Mg, Na, S, Ti, Mn, Zn, Cu, V, Cr, Co, Ba, Pb, U)
4) F^-, Cl^-, NO_3^-, SO_4^{2-}, Na^+, NH_4^+, K^+, Mg^{2+}, Ca^{2+}
5) Total column ozone
6) $PM_{1,2.5,10}$, size distribution (0.5-20 μm), Condensation Particle Counter (0.01-3 μm)
7) $PM_{1,2.5,10}$, size distribution (0.5-20 μm)
8) Vertical profile of ozone measured by ozone-sonde
9) AOD, vertical profiles of backscattering coefficient, depolarization ratio, and color ratios

methodologies are secured and applied, e.g. greenhouse gas isotopes, aerosol chemical species, and volatile organic compounds (VOCs). To enhance the effectiveness and application of the long-term measurements within GAW, KMA cooperates with the atmospheric measurement networks worldwide along with focusing on the quality assurance and control.

World Calibration Center for SF$_6$

World Calibration Centers (WCC), one of the GAW central facilities, maintain calibration standards and provide instrument calibrations and training to the stations, that is, link observations to World Reference Standards and ensure networks comparability and compatibility through inter-comparison campaign and regular audits (see Figure 2). World Calibration Center for SF$_6$ (WCC-SF$_6$) was designated to be established in KMA in 2012, and has been operated since 2013. WCC-SF$_6$ conducts the missions for the traceability and compatibility of the SF$_6$ measurement in the GAW network. The main tasks of the WCC-SF$_6$ are to; 1) disseminate the tertiary standard gas allowing to maintain laboratory and transfer standards that are traceable to the primary standards, 2) conduct regular calibrations and performance audits at GAW stations using transfer standards, 3) run technical training and educational courses to provide the theoretical/technical help for the stations, and 4) develop the measurement guideline and quality control procedures, and ensure the traceability of the measurement to the corresponding primary standard. In practice the missions has been initiated and first applied to the Korean domestic stations since 2014. We have a plan to cover the stations at the Asia-Pacific region in 2015. We hope to get a regional education and training center for atmospheric SF$_6$ measurement established in KMA.
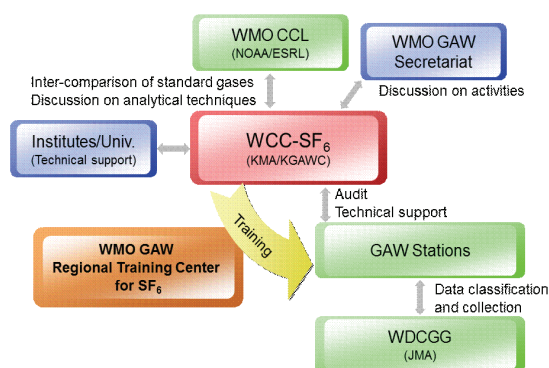

Figure 2

Schematic on operation of World Calibration Center for SF$_6$ (WCC-SF$_6$). KGAWC cooperates with institutes and universities for it, e.g. Korea Research Institute of Standards and Science (KRISS). WMO Central Calibration Laboratory (CCL) for SF$_6$ is managed by Earth Science Research Laboratory (ESRL) in NOAA. World Data Centre (WDCGG) is managed by Japan Meteorological Agency (JMA).

Asia-Pacific GAW workshop on Greenhouse Gases

The Asia-Pacific GAW Workshop on Greenhouse Gases has annually been held by KMA since 2009. It provides a good opportunity to share our knowledge on greenhouse gases measurements in the Asia and Pacific region.

More than 60 participants were in the workshop, 2014. The workshop is in connection with the technical training course in part of the WCC-SF$_6$ activities.

References

[1] World Meteorological Organization, Global Atmosphere Watch measurement guide, WMO GAW report No. 143, WMO TD No. 1073, July 2001.

[2] World Meteorological Organization, WMO/ GAW aerosol measurement procedures: Guidelines and recommendations, WMO GAW report No. 153, WMO TD No. 1178, September 2003.

Observational constraints on the global methane budget

Edward J. Dlugokencky[1*], Andrew Crotwell[1,2], Ken Masarie[1],
James W.C. White[3], Patricia Lang[1], and Molly Crotwell[1,2]

Introduction

The atmospheric burden of CH_4 has increased by a factor of 2.5 since 1750, contributing 0.5 W m^{-2} to total radiative forcing by long-lived greenhouse gases (2.90 W m^{-2} in 2013). When equal masses of CH_4 and CO_2 are emitted to the atmosphere, the integrated impact of CH_4 on climate over 100 years is 28 times greater than CO_2. Methane's atmospheric chemistry affects background air quality and contributes an additional ~0.2 W m^{-2} indirect forcing through production of tropospheric O_3 and stratospheric H_2O. Studies of Earth's paleoclimate show that changes in CH_4 emissions from tropical and Arctic wetlands have likely contributed a positive feedback to climate during transitions from glacial to interglacial periods. There is reasonable cause for concern that a similar climate feedback from CH_4 could become important in response to recent anthropogenic forcing of climate. Because atmospheric CH_4 has a relatively short life time, ~9 yr, reducing its emissions is considered a potential approach to slowing the rate of increasing radiative forcing. In fact, reductions in emissions from many anthropogenic sources would be cost-effective. However, the effectiveness of emissions mitigation may be over-estimated by bottom-up inventories, so emission reductions must be verified through atmospheric observations. Also, reductions in anthropogenic emissions may be offset by increased emissions from natural sources such as Arctic wetlands as they respond to changing climate.

NOAA has been measuring the global distribution of atmospheric CH_4 since 1983 using

1. National Oceanic and Atmospheric Administration, Earth System Research Laboratory, Global Monitoring Division, Boulder, Colorado, USA
2. CIRES, Univ. of Colorado, Boulder, CO, USA
3. INSTAAR, Univ. of Colorado, Boulder, CO, USA

GAW practices for measurement quality first adopted by Dave Keeling in the 1950s. These CH_4 data provide important constraints on methane's large-scale budget and how it is changing with time. Key temporal features in the data are a long-term decrease in growth rate from 1983 to 2006, significant inter-annual variability in the rate of increase (which test our understanding of CH_4 budget processes), and a renewed increase starting in 2007. Observed spatial patterns in atmospheric CH_4 also constrain CH_4's global budget. Here we look at more than 30 years of CH_4 measurements and try to understand the processes behind these changes.

Sampling and analysis methods

Discrete air sample pairs are collected approximately weekly in 2.5 L flasks from ~60 sites (as of 2014) in NOAA's cooperative global air sampling network[1] (also http://www.esrl.noaa. gov/gmd/ccgg/flask.html). Flasks are flushed and pressurized to ~1.2 atm with a portable sampler. Samples are collected under conditions when air is representative of large, well-mixed volumes of the atmosphere to facilitate comparison with simulations from chemical transport models that have relatively large grid-scale resolution. In addition to measurement of CH_4 by GC with flame ionization detector (FID), other species measured by NOAA with by collaborators at the University of Colorado are CO_2, N_2O, SF_6, H_2, CO, C and O isotopes of CO_2, VOCs, and C and H

isotopes of CH_4 (in a subset of samples). FID response is calibrated with standards on the WMO GAW mole fraction scale maintained at NOAA and reported as dry-air mole fractions (CH_4 data path:ftp://aftp.cmdl. noaa.gov/data/ trace_gases/ch4/flask/surface/). To calculate zonal means representative of large spatial scales, data from a subset of our globally-distributed remote boundary layer sites were fitted with curves to smooth variability with periods less than ~40 days.[1] Synchronized points were extracted from these curves at approximately weekly intervals and smoothed as a function of latitude to define an evenly spaced matrix of surface CH_4 mole fractions as a function of time and latitude. This matrix was used to calculate global and zonal averages.

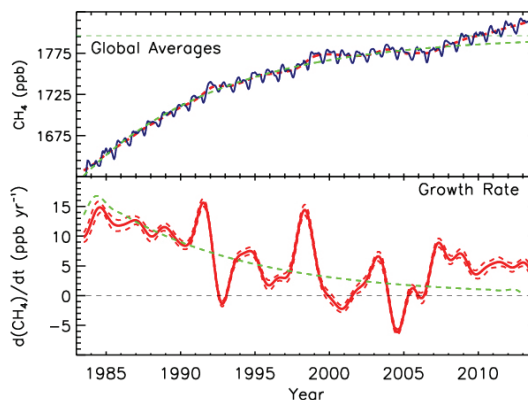## Long-term changes in atmospheric CH_4

Figure 1

Top: CH_4 dry-air mole fractions (blue), deseasonalized trend (red), and approach to steady state (green). Bottom: Instantaneous growth rate (red); time derivative of trend curve.

Atmospheric CH_4 dry air mole fractions at weekly resolution are plotted in blue in the top panel of Figure 1. The trend, determined by subtracting the seasonal cycle from the global means, is in red. In the bottom panel, the instantaneous growth rate is plotted in red with uncertainties (68% confidence interval) determined from a Monte Carlo method. The trend (growth rate) is directly related to the imbalance between emissions and losses, so it is an important constraint on the global CH_4 budget. From the start of the measurement program in 1983 through 2006, the rate of increase (growth rate) of atmospheric CH_4 was decreasing, despite significant interannual variability, which is discussed in detail below.

This feature is an important constraint on the evolution of the atmospheric CH_4 budget, so it is vital we try to understand its causes. The change in atmospheric CH_4 burden is given by: $d[CH_4]/dt=E-[CH_4]/\tau$ (1), where $[CH_4]$ is the global CH_4 burden, E is total global emissions, and τ is the atmospheric CH_4 lifetime. This equation can be rearranged to calculate annual emissions from the observed global annual increase and burden, and an estimate of the lifetime from the literature (9.1±0.9 yr [2]), as shown in Figure 2 in blue symbols. A linear fit to 1984 to 2006 gives no trend, 0.0±0.6 Tg CH_4 yr^{-1} (uncertainty is 95% c.i.). For comparison, emissions estimates from EDGAR (Emissions Database for Global Atmospheric Research) are plotted in filled red triangles; open triangles are an ex-

trapolation based on global increases in fossil fuel use. Agreement in emissions trends between measurement-based and inventory-derived emissions is poor. The inventory clearly over-estimates the trend in emissions. Constant emissions from 1984-2006 indicate that, if the CH_4 lifetime has been approximately constant, atmospheric CH_4 is approaching steady state.

At steady state, $d[CH_4]/dt=0$ and $E=[CH_4]_{ss}/\tau$. The approach to steady state for this system is defined by[3]:

$$[CH_4](t)=[CH_4]_{ss}-([CH_4]_{ss}-[CH_4]_0)e^{-t/\tau} \quad (2)$$

Subscripts are "$_{ss}$" for the steady-state value of CH_4 and "$_0$" for CH_4 at the start of the time series; τ is the CH_4 lifetime. A fit of Equation 2 to the global means from 1984 through 2006 is plotted in green in Fig. 1, and its time-derivative is shown with the observed growth rate in the bottom panel.
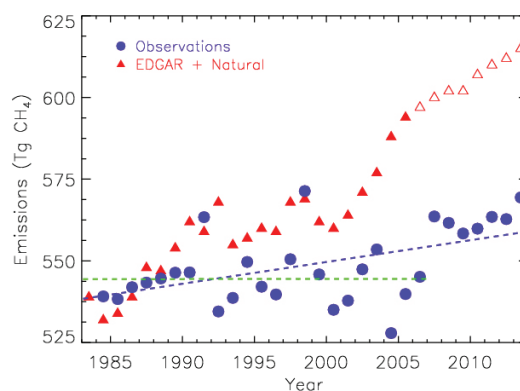

Figure 2

Global CH_4 emissions calculated from Equation 1 and $\tau=9.1$ yr are plotted in blue. Green line is a linear fit to emissions, 1984-2006 (0±0.6 Tg CH_4 yr^{-1}). Including 2007-2013 (blue line), the trend is 0.7±0.4 Tg yr^{-1}. Red triangles are emissions from EDGAR (plus fixed natural emissions), extrapolated (open symbols) based on global fossil fuel use.

We obtain $[CH_4]_{ss}$=1996 ppb (horizontal green dashed line) and τ=9.4 yr, very close to the recent literature estimate.

After a decade of near-zero growth, atmospheric CH_4 began increasing again globally in 2007,[4, 5] as shown in Figure 1, and globally averaged CH_4 has deviated from the steady state regime. This is discussed further below.

Short-term changes in atmospheric CH_4

Superimposed on top of the long-term approach to steady state are significant inter-annual variations in CH_4 growth rate that are often related to changes in specific processes. In 1991, the eruption of Mt. Pinatubo injected ~20 Mt SO_2 and 3-5 km^3 ash into the upper troposphere and lower stratosphere. We calculated the photochemical impacts of direct UV absorption by SO_2, and found a reduction in $O(^1D)$ formation (a precursor to OH) of ~12% immediately after the eruption, and that $O(^1D)$ production was perturbed for up to a year after the eruption.[6] Less $O(^1D)$ production resulted in ~8% less OH, which decreased CH_4's chemical sink and caused the anomalous increase in growth rate. In 1992, the growth rate of atmospheric CH_4 decreased dramatically; while decreased tropospheric temperature resulting from less solar insolation reaching Earth's surface likely affected CH_4 emissions from natural wetlands, the abruptness and persistence of the change indicated a source easily affected by human activities such as fossil fuel exploitation.[7] Analysis of changes in spatial patterns of atmospheric CH_4 suggested there was a permanent decrease in emissions after the economic restructuring in the former Soviet Union.[8] In 1997 and 1998, atmospheric CH_4's growth rate rapidly and temporarily increased again. Using an adaptation of a global wetland process model, we showed that the growth rate was likely affected by changes in emissions from natural wetlands and biomass burning.[9]

Changes since 2007

Starting in 2007, the growth rate rose again after remaining near-zero (averaging 0.5 ppb yr^{-1}) from 1999-2006, causing concern that Arctic permafrost and shallow ocean hydrates were responding to warming. We considered various possibilities for the increase. An increase in CH_4 emissions from biomass burning was not consistent with CO and $\delta^{13}C(CH_4)$ measurements from the same air samples analyzed for CH_4. Changes in observed spatial patterns indicate the increase was driven by increased Arctic and tropical emissions.[5] Likely drivers for increased emissions in 2007 are anomalously high temperatures and precipitation in wetland regions, particularly in the Arctic and tropics. Since 2007, atmospheric CH_4 continues to increase at ~6 ppb yr^{-1}. Despite continued warmth in the Arctic, inversions of atmospheric chemical

transport models suggest emissions there returned to normal levels in 2008. The causes of the continued global increase are not clear, but greater than average precipitation in tropical wetland regions and increased anthropogenic emissions are likely the largest contributors consistent with observed decreases in $\delta^{13}C(CH_4)$. Unfortunately, the current observing network for atmospheric CH_4 abundance is not sufficient to determine with certainty the causes of the CH_4 increasesince 2007. This points to the critical need for a denser network of observations, along with additional constraints on the atmospheric methane budget such as observations of methane isotopic composition.

References

[1] Dlugokencky, EJ, *et al*. (1994), The growth rate and distribution of atmospheric methane, J. Geophys. Res., 99 (D8), 17021−17043, *doi:10.1029/ 94JD01245*.

[2] Prather, MJ, CD Holmes, and J Hsu (2012), Reactive greenhouse gas scenarios: Systematic exploration of uncertainties and the role of atmospheric chemistry, Geophys. Res. Lett., 39, L09803, *doi:*10.1029/2012GL051440.

[3] Dlugokencky, EJ, KA Masarie, PM Lang, and PP Tans (1998), Continuing decline in the growth rate of atmospheric methane, *Nature*, 393, 447−450, *doi:10.1038/30934*.

[4] Rigby, M *et al.* (2008), Renewed growth of atmospheric methane, Geophys. Res. Lett., 35, *L22805, doi*:10.1029/2008GL 036037.

[5] Dlugokencky, EJ *et al*. (2009), Observational constraints on recent increases in the atmospheric CH_4 burden, Geophys. Res. Lett., 36, *L18803, doi*:10.1029/2009 GL039780.

[6] Dlugokencky, EJ, *et al*. (1996), Changes in CH_4 and CO growth rates after the eruption of Mt. Pinatubo and their link with changes in tropical tropospheric UV flux, Geophys. Res. Lett.,23(20), 2761−2764, doi:10.1029/96GL02638.

[7] Dlugokencky, EJ, *et al.* (1994), A dramatic decrease in the growth rate of atmospheric methane in the Northern Hemisphere during 1992, Geophys. Res. Lett., 21, 45−48.

[8] Dlugokencky, EJ, *et al.* (2003), Atmospheric methane levels off: Temporary pause or a new steady-state? Geophys. Res. Lett., 30(19), 1992, *doi:*10.1029/ 2003GL018126.

[9] Dlugokencky, EJ, *et al*. (2001), Measurements of an anomalous global methane increase during 1998, Geophys. Res. Lett., 28,499−502, *doi:*10.1029/2000GL 012119.

A new JMA program of operational aircraft observation for atmospheric CO$_2$, CH$_4$, CO, and N$_2$O in the mid-troposphere

Masaomi TAKAHASHI[1*], Yuji ESAKI[1], Yukio FUKUYAMA[1], Shinya TAKATSUJI[1], Hiroaki FUJIWARA[1], Tomoki OKUDA[1], Kohshiro DEHARA[1], Yoki MORI[1], Hidekazu MATSUEDA[2], Yousuke SAWA[2], Kazuhiro TSUBOI[2], and Yosuke NIWA[2]

Introduction

In order to better understand the spatial and temporal variations of the greenhouse gas fluxes in Asia and their contributions to the global carbon cycle, the Japan Meteorological Agency (JMA) has carried out an operational aircraft observation as a new atmospheric monitoring activity since 2011. In this paper, by analyzing results of the JMA aircraft observation, seasonal variations of greenhouse gases in the mid-troposphere over the western North Pacific are presented. Furthermore, a vertical profile variation of methane (CH$_4$) mole fractions over Minamitorishima is discussed for the summer-autumn season.

Sampling and analysis methods[1]

The JMA aircraft observation is carried out by using a cargo aircraft C-130H of the Japan Ministry of Defense, which flies regularly from Atsugi Base (35°27' N, 139°27' E) in Kanagawa prefecture near Tokyo to Minamitorishima (24°17' N, 153°59' E) once a month (Figure 1). In one flight, 18 flask air samples are collected during a cruising section at an altitude of about 6km over the western North Pacific (corresponding to the mid-troposphere) with an interval of about 100km, and 6 flask air samples are collected during a descending section to Minamitorishima with an interval of about 1km.

1. Japan Meteorological Agency, Tokyo, Japan
2. Meteorological Research Institute, Tsukuba, Japan

In the cargo room of the aircraft C-130H, flask air sampling is manually carried out by using a modified diaphragm pump. A flask used in the aircraft observation has an internal volume of about 1.7 L and is made of titanium with a thickness of 1.2mm. Fresh air outside the aircraft is fed into the cargo room through the air-conditioning system in the aircraft and is collected into each flask by pressurizing it to about 0.4 MPa by using the diaphragm pump. Coarse dust and water vapor in the fresh air are removed by a stainless steel filter (60μm mesh size) and a dryer tube (packed with carbon dioxide (CO_2)-saturated magnesium perchlorate) before the fresh air is collected into each flask.

After a flight, mole fractions of four trace gases (CO_2, CH_4, carbon monoxide (CO), and nitrous oxide (N_2O)) in flask air samples are measured at the JMA headquarters in Tokyo. An automated measurement system was newly developed by a collaborative work of Meteorological Research Institute and JMA to achieve high-precision measurements for all the trace gases (Tsuboi et al., 2013). As Table 1 shows, this system consists of the following four analyzers: a non-dispersive infrared (NDIR) analyzer for CO_2, a wavelength-scanned cavity ring-down spectroscopy (WS-CRDS) analyzer for CH_4, a vacuum ultraviolet resonance fluorescence (VURF) analyzer for CO, and an off-axis integrated cavity output spectroscopy (ICOS) analyzer for N_2O. The traceability of measurements to the World Meteorological Organization (WMO) mole fraction scale for each trace gas is ensured because the multi-species working standard gases used for the flask air sample measurements are calibrated by the JMA primary standard gases, of which scales are propagated from the National Oceanic and Atmospheric Administration (NOAA) Central Calibration Laboratory.
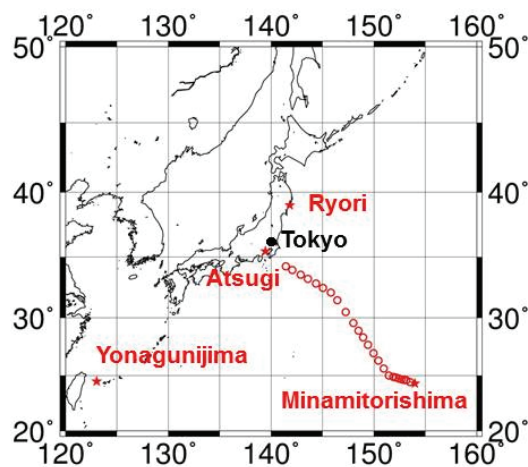

Figure 1

Flask sampling points of the aircraft C-130H observation between AtsugiBase and Minamitorishima (red opened circles).

Table 1. Analyzers used in the JMA automated measurement system for flask air samples[1]

Trace gas	Analyzer	Precision	Standard gas scale
CO_2	NDIR (LI-COR, LI-7000)	0.014 ppm	WMO X2007
CH_4	WS-CRDS (Picarro, G2301)	0.26 ppb	NOAA 04
CO	VURF (Aero-Laser, AL5002-AIR)	0.28 ppb	WMO CO X2004
N_2O	off-axis ICOS (Los Gatos Research, DLT100)	0.07 ppb	NOAA 2006A

Results and discussion

Figure 2 shows temporal variations of mole fractions of CO_2, CH_4, CO, and N_2O observed at the altitude of about 6km over the western North Pacific during the flights from Atsugi Base to Minamitorishima. The mole fractions of CO_2, CH_4, and N_2O show increasing trends and these trends are similar to those observed at Minamitorishima ground-based station (MNM). Moreover, the CO_2 mole fraction shows a distinct seasonal cycle with an increase during winter-spring and a decrease during summer-autumn. Amplitude of this seasonal cycle is about 10 ppm, which is slightly smaller than that of MNM. On the other hand, the CO mole fraction doesn't show a distinct increasing nor decreasing trend.

As shown in Figure 2, much higher CH_4 mole fractions than the regression line were occasionally observed in summer (Niwa et al., 2014). In order to compare the CH_4 mole fraction in the mid-troposphere to that observed at the surface, a temporal variation of CH_4 mole fraction observed at MNM is shown in Figure 3. The CH_4 mole fractions in Figure 2 are also superimposed on Figure 3. The CH_4 mole fraction at MNM shows a distinct seasonal cycle with an increase during winter-spring and a decrease during summer-autumn. Furthermore, Figure 3 indicates that the CH_4 mole fractions during summer at the altitude of about 6km are occasionally much higher than those at MNM.
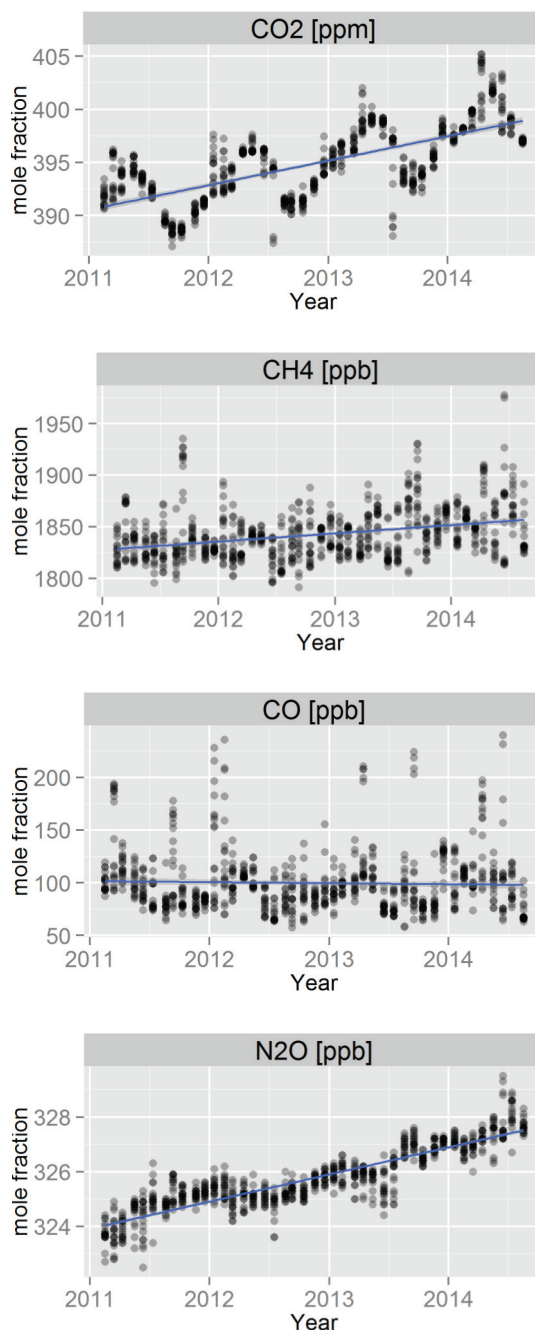

Figure 2

Temporal variations of mole fractions of CO_2, CH_4, CO, and N_2O observed at the altitude of about 6km over the western North Pacific during the flights from Atsugi Base to Minamitorishima. Semi-transparent black circles show mole fractions of trace gases. Solid blue lines denote the regression lines.

Figure 3

Temporal variations of observed CH_4 mole fractions. Red dots show the CH_4 mole fractions at MNM, and semi-transparent black circles show the CH_4 mole fractions in the mid-troposphere.

Figure 4 shows vertical profiles of CH_4 mole fractions observed over Minamitorishima in each month. The observation results indicate that the CH_4 vertical profile varies seasonally. The CH_4 mole fraction decreases with the increase of altitude during winter-spring because the CH_4 sources exist at the surface and the atmosphere is well stratified during winter-spring. However, the CH_4 mole fraction increases as the altitude increases during summer-autumn.
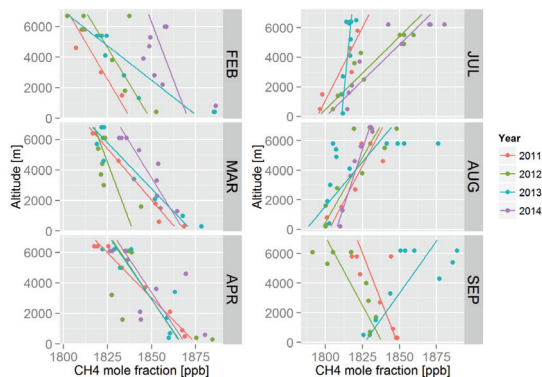

Figure 4

Vertical profiles of CH_4 mole fractions observed over Minamitorishima in each month (left: winter to spring, right: summer to autumn). Solid lines denote the regression lines.

Figure 5 shows 168 h back-trajectories of the air masses over Minamitorishima on July 2014 as an example of a back-trajectory of the air masses over Minamitorishima during summer-autumn. The initial time is 04 UTC 14 July 2014 and it corresponds to the time at which the aircraft observation over Minamitorishima on July 2014 was carried out. Figure 5 indicates that the oceanic air masses were transported from the west of Hawaii to Minamitorishima in the lower troposphere while the continental air masses were transported from the Asian continent to over Minamitorishima in the mid-troposphere. This result suggests that the CH_4 mole fractions at the mid-troposphere were originated from the Asian continent during summer-autumn.

Figure 6 shows correlation plots for mole fractions of CO and CH_4 observed by the aircraft C-130H during summer-autumn and during winter-spring. The regression slope during summer-autumn is steeper than that during winter-spring, indicating that the CH_4 mole fraction is larger during summer-autumn than during winter-spring in the case of the same CO mole fraction level. This result suggests that the CH_4 mole fractions in the mid-troposphere over the western North Pacific during summer-autumn is contributed by the biogenic emissions in Asia such as wetlands and rice paddies stimulated by summer temperature increase. The detailed analyses about this result are given by Niwa et al. (2014).[2]
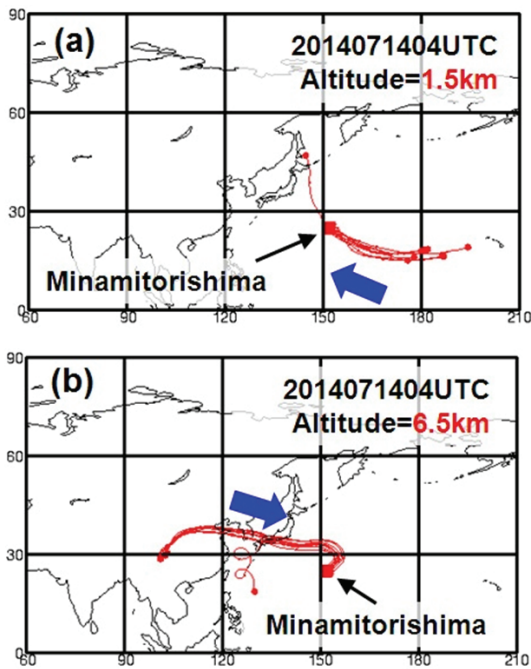
Figure 5

Seven-day (168h) back-trajectories of the air masses over Minamitorishima on 14 July 2014 ((a) lower troposphere (at 1.5km) and (b) mid-troposphere (at 6.5km)).
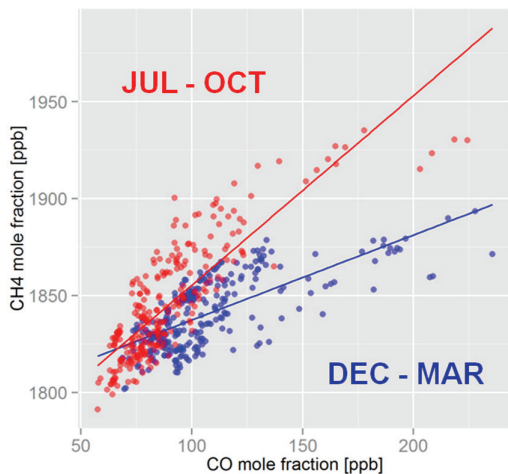

Figure 6

Correlation plots for CO-CH$_4$ observed by the aircraft C-130H during summer-autumn (July-October, red) and during winter-spring (December-March, blue). Solid lines denote the regression lines.

Conclusion

In order to better understand the spatial and temporal variations of greenhouse gas fluxes in Asia and their contributions to the global carbon cycle, JMA has carried out an operational aircraft observation since 2011.

Over Minamitorishima, the observation results showed that the CH$_4$ vertical profile varied seasonally. Specifically, the CH$_4$ mole fraction decreases with the increase of altitude during winter–spring, meanwhile it increases as the altitude increases during summer–autumn. The observed vertical profile during summer–autumn suggests that CH$_4$ rich air masses influenced by increased biogenic sources in the Asian continent are transported to over the western North Pacific.

References

[1] Tsuboi, K., H. Matsueda, Y. Sawa, Y. Niwa, M. Nakamura, D. Kuboike, K. Saito, H. Ohmori, S. Iwatsubo, H. Nishi, Y. Hanamiya, K. Tsuji, and Y. Baba (2013), Evaluation of a new JMA aircraft flask sampling system and laboratory trace gas analysis system, *Atmos. Meas. Tech., 6, 1257–1270, doi:10.5194/amt-6-1257-2013*.

[2] Niwa, Y., K. Tsuboi, H. Matsueda, Y. Sawa, T. Machida, M. Nakamura, T. Kawasato, K. Saito, S. Takatsuji, K. Tsuji, H. Nishi, K. Dehara, Y. Baba, D.

Kuboike, S. Iwatsubo, H. Ohmori, and Y. Hanamiya (2014), Seasonal Variations of CO_2, CH_4, N_2O and CO in the Mid-Troposphere over the Western North Pacific Observed Using a C-130H Cargo Aircraft, *J. Meteorol. Soc. Japan, 92(1), 55－70, doi:10.2151/jmsj.2014-104.*

A decade of greenhouse gas monitoring activities in Bukit Kototabang, Indonesia

Alberth Christian Nahas[*]

As of the end of 2013, the greenhouse gas (GHG) monitoring activities at the Global GAW Station Bukit Kototabang (0.20194°S, 100.31805°E, 864 m a.s.l.) has reached a decade of observation. During the course of this period, mole fractions of the three major GHGs: CO_2, CH_4, and N_2O have indicated an incremental trend by 5.1%, 1.8%, and 2.5% respectively. These increasing percentages, however, are overwhelmingly surpassed by a 46% rise of SF_6 mole fractions indicating the fastest growth of all GHGs. Meanwhile, all gases have reached the newest highs in 2013 with the annual mole fractions of CO_2 at 392.1 ppm, CH_4 at 1839.3 ppb, N_2O at 327.1 ppb and SF_6 at 7.9 ppt. Moreover, last year is also marked with the highest increase of year-on-year CO_2 mole fractions; between the period of 2012 and 2013, CO_2 has increased by 1.7%, which is slightly more than four times larger than its annually averaged growth rate during the period 2004-2012. This significance increase can be related to extensive fire episodes over a number of areas in Sumatra, occurred in February-March and in June-August 2013. It has been suggested that besides the health and environmental impacts, wildfires also contributed to a considerable amount of CO_2 emissions,[1] which can be counted for massive release of the gas in a short period.

Development of measurement programs

In January 2004, the GHG activities in Bukit Kototabang was started with the installation of

the NOAA Flask Sampling that collected the ambient air into two 2.5-liter flasks containing ambient air taken from a 32 m height inlet. With this installation, Bukit Kototabang is the first site in Indonesia that has an ongoing GHG measurement program. Prior to this program, there were several monitoring programs, including one in Bukit Kototabang installed by Kyoto University to measure CO_2 mixing ratios in the early 2000s. Such programs, however, were mainly focused for a short-term research project and were generally terminated within a couple of years.

The NOAA Flask Sampling was the only GHG measurement program conducted in Bukit Kototabang until 2008. In October 2008, a Picarro G1301 $CO_2/CH_4/H_2O$ analyzer was installed at the station. The instrument provides a continuous measurement, allowing the observers to get near-real time data. A year later, an automated inlet and calibration system were added to support the measurement of the existing Picarro. The system, which was installed by MeteoSwiss and WCC-Empa, enables the instrument to automatically measure the GHG mixing ratios of ambient air from three height levels, as well as to perform calibration up to three different concen -trations. In November 2011, the GHG measurement (CO_2 and CH_4) was included for the first time in the GAW system and performance audit by WCC-Empa. Details on the audit results can be further perused in the report provided elsewhere.[2]

The latest GHG monitoring instrument added in Bukit Kototabang was Thermo IRIS4600 N_2O Analyzer, which was installed in June 2013. Similar to the Picarro, this analyzer measures near-real time N_2O mixing ratios from the ambient air. The analyzer also shares the same inlet and calibration system with the Picarro for supporting the automated ambient air/standard gas intake. The performance of this analyzer, along with the overall GHG monitoring program, was examined in the last system and performance audit by WCC-Empa, and the results were recently released in a report.[3]

Results

Over the last 10 years, the GHG mixing ratios measured at Bukit Kototabang have been used for representing the profile of GHGs in a remote tropical rainforest area in Indonesia. As mentioned earlier in this article, all measured GHGs have been increasing with different rates. Table 1 summarizes the annual abundance of four GHGs for the period 2004-2013.

As indicated in Table 1, the increment trends of GHG mixing ratios are observed in Bukit Kototabang. This trend is of particular large for SF_6 that its concentration in 2013 has increased by almost 50 percent. Meanwhile, the mean absolute increase of GHG in Bukit Kototabang is slightly larger for CO_2 and N_2O, with the rate for CH_4 is close to that measured globally.

Table 1. The annual abundance of CO_2, CH_4, N_2O and SF_6 measured at the Global GAW Station Bukit Kototabang. Figures in the brackets are taken from the latest WMO GHG Bulletin[4] to compare the results with the global trend. The global relative abundance of CO_2 is calculated from the global CO_2 mixing ratios reported by the NOAA/ESRL Global Monitoring Division

Parameter	CO_2	CH_4	N_2O	SF_6
Abundance in 2013	392.1 ppm (396 ppm)	1839.3 ppb (1824 ppb)	327.1 ppb (325.9 ppb)	7.9 ppt
2013 abundance relative to year 2004	105% (105%)*	102%	103%	146%
Mean annual absolute increase during the period 2004-2013.	2.12 ppm/yr (2.07 ppm/yr)	3.7 ppb/yr (3.8 ppb/yr)	1 ppb/yr (0,82 ppb/yr)	0.31 ppt/yr

Focusing on CO_2 and CH_4, Figure 1 shows CO_2 and CH_4 trends from the period 2004-2013. The seasonal trend for these gases can be observed by the fluctuated mixing ratios from consecutive periods. During the northern hemisphere winter or the wet months in Bukit Kototabang, the mixing ratios of the two gases are relatively higher than other periods.
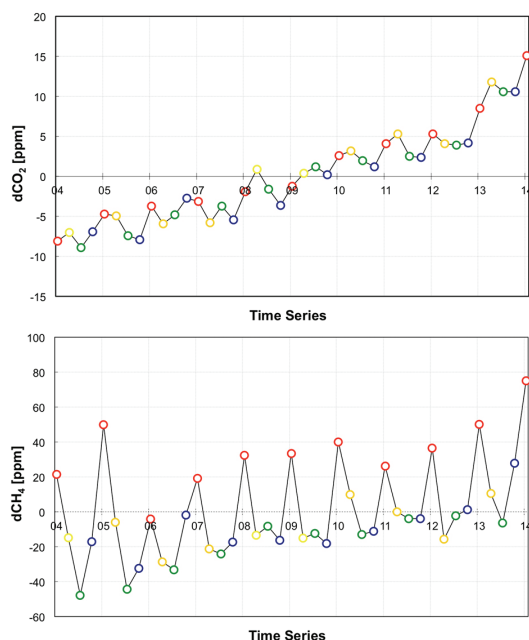

Figure 1

Seasonal trends of CO_2 (top) and CH_4 (bottom) relative to the 2004-2013 annual average. Each color represents a 3-monthly period, DJF = red, MAM = yellow, JJA = green and SON = blue.

Impacts of wildfire events

Some regions in Indonesia are prone to the occurrence of wildfires due to extreme dry periods, fuelled by extensive peatlands and slash-and-burn farming activities. One of these areas is Sumatra, particularly the peat dominated areas in the east coast of the island. Even though Bukit Kototabang is not located near to the hotspots, the air from the fire-affected areas transported to the site, bringing the pollutant and the emitted carbon to the station. Not only did the polluted air degrade the air quality, the CO_2 mixing ratios during the wildfire events also increased considerably.

Figure 2 provides a snapshot of the monthly CO_2 mixing ratio differences in a consecutive year in the period 2004-2013. The periods where the fire episodes were present are marked with relatively high CO_2 mixing ratios. These periods were commonly associated with the dry periods that have increased the probability of fire occurrence. However, CO_2 mixing ratios in each month of 2013 were higher than the previous year, even

though this year was not an El Niño nor DMI-affected year. A recent study suggests that the ongoing deforestation taken place in the several areas in Sumatra is responsible for the fire events during a non-drought year.[4]
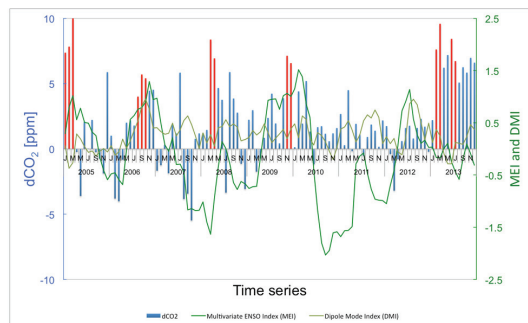

Figure 2

The monthly difference of CO_2 mixing ratio in Bukit Kototabang over the period 2004-2013. The difference is calculated from the same month of the consecutive year (i.e. the mixing ratio in January 2005 is obtained from the difference between mixing ratio in January 2004 and January 2005, and so on). The red bars represent the months in which the wildfires were notably detected. The green and light green lines indicate the Multivariate ENSO Index (MEI) and Dipole Mode Index (DMI), respectively. These indices are often related to the dry period in Sumatra.

Further directions

In comparison to other sites in different countries, a 10-year period of GHG monitoring activities in Bukit Kototabang, Indonesia is much shorter. The number of parameters measured, as well as measurement techniques, is also somewhat limited to give an overall view of what the GHG profile in the site looks like. In addition, some technical and logistical challenges are the major factors that are hindering the activities. Nevertheless, the activities in Bukit Kototabang is important,

not only to fill the gap of GHG monitoring blank spots in the equatorial region, but also to provide valuable data for GHG- and climate-related research. Therefore, the GHG monitoring activities performed in Bukit Kototabang should be continued for coming decades, while attempts to overcome the challenges remain in place.

References

[1] Langmann B (2014). The Impact of Vegetation and Peat Fire Emissions in Indonesia on Air Pollution and Global Climate, *Asian Journal of Water, Environment and Pollution* 11(1): 3-11.

[2] Zellweger *Cet al.* (2011). System and Performance Audit of Surface Ozone, Methane, Carbon Dioxide and Carbon Monoxide at the Global GAW Station Bukit Kototabang, Indonesia, November 2011, *WCC-Empa Report 11/4*.

[3] Zellweger *Cet al.* (2014), System and Performance Audit of Surface Ozone, Methane, Carbon Dioxide, Nitrous Oxide and Carbon Monoxide at the Global GAW Station Bukit Kototabang, Indonesia, May 2014, *WCC-Empa Report 14/1*.

[4] Gaveau DLA, *et al.* (2014). Major atmospheric emissions from peat fires in Southeast Asia during non-drought years: evidence from the 2013 Sumatran fires. *NatureScientific Reports* 4. doi:10.1038/srep06112.

Atmospheric CO₂ observations and the Indian Monsoons

Yogesh K. Tiwari[1*], Ramesh K. Vellore[1], K. Ravi Kumar[1], Marcel van der Schoot[2], and Chun-Ho Cho[3]

Most of the atmospheric CO_2 investigations conducted over the Indian subcontinent are based on aircraft measurements or from the model simulations and not based on ground-based atmospheric observations.[1] Despite the paucity of surface observations in this region, recent studies have revealed the general connections between GHG's and the Indian summer monsoon (ISM).[2, 3] In response to larger scale land-sea thermal contrast, the largest volume of precipitation over the Indian subcontinent is observed during the summer and winter monsoon periods [June to September (JJAS) in summer and December to February (DJF) in winter].[4] Monsoon core regions in the summertime are defined over the Indo-Gangetic Plains (IGP) region, central part of the subcontinent and the mountainous west coast of India, as well as over the south-ern part of peninsular India during wintertime (refer Figure 1, left panels).
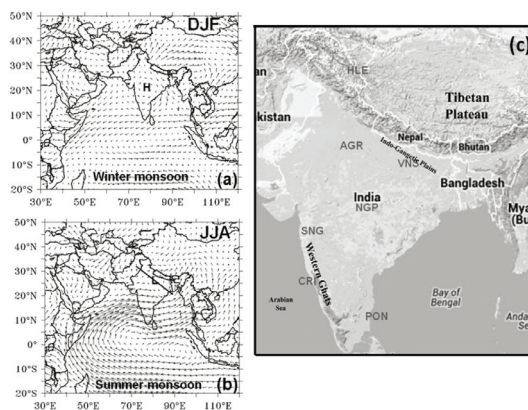
Figure 1

(a) & (b) NCEP-diagnosed 850 hPa mean winds, (c) Locations of the sites Sinhagad (SNG), Cape Rama (CRI), Nagpur (NGP), Pondicherry (PON), Agra (AGR), Varanasi (VNS), and Hanle (HLE) over the Indian subcontinent referenced in this study (source: https://maps.google.co.in).

From a meteorological perspective, the maritime transport mechanisms are essential for

1. Centre for Climate Change Research, Indian Institute of Tropical Meteorology, Pune, India
2. Centre for Australian Weather and Climate Research, CSIRO Marine & Atmospheric Research, Australia
3. National Institute of Meteorological Research, Korea

source region CO_2 estimates as the southwesterly summer monsoon from the Arabian Sea initially reaches the coastal regions in the western part of India during the ISM (Figure 1, left panel). The influence of the continental source regions during the ISM cannot be disregarded due to the winter monsoon wind reversal regime. Therefore, quantification of the GHG's source/sink regions and the atmospheric residence times over the oceanic and continental regions is necessary in the context of understanding the atmospheric carbon cycle in this region.

The objective of the present study is to investigate the impact of the Indian summer and winter monsoon circulations on atmospheric CO_2 observations at two ground-based air sampling sites located in western India SNG and CRI (refer Figure 1, right panel). This is supported by atmospheric transport modeling results to provide some insights into CO_2 variability over the subcontinent. Routine air sampling at SNG, collected from a 10 meter meteorological tower at weekly intervals, has been operational since November 2009. Glass flasks were analyzed at IITM Pune India.[5] On the other hand, routine air sampling at CRI commenced in February 1993 and continued until October 2002, and resumed again in July 2009. Glass flasks sampled at CRI were analyzed at the gas lab CSIRO Australia.[6]

Two models are used in this study to analyze the spatial distribution of CO_2 and the identification of source regions. The models are: (i) Lagrangian particle dispersion model FLEXPART[7] and (ii) Carbon Tracker.[8, 9] FLEXPART is a comprehensive atmospheric transport modeling tool originally designed for air quality studies to investigate the long-range and meso-scale dispersion of pollutants from point sources. A back-trajectory analysis from the FLEXPART model provides a good basis for the assessment of source-receptor relationships. Carbon Tracker (CT) is a global reanalyzed product used to synthesize the spatio-temporal variability of CO_2. The atmospheric transport is simulated using the global two-way nested Transport Model version 5 (TM5) which is forced by the time-varying meteorology from the European Center for Medium Range Weather Forecast (ECMWF) reanalysis products. The model configuration has a regional domain in the horizontal centered over Asia at $1° \times 1°$ resolution and 34 levels in the vertical hybrid-sigma coordinate. Fluxes are provided based on fossil fuel use, wildfire, vegetation and the oceans. We used CT-Asia CO_2 concentration products simulated at NIMR Korea for the period 2000-2010.

Figure 2 top panel (a to d) show the FLEXPART simulated particle back-trajectories reaching the surface level at SNG during the months of January and July. The particles predominantly showed an eastward mass transport over larger distances of continental length scales as well as gently descending from the upper to lower troposphere.
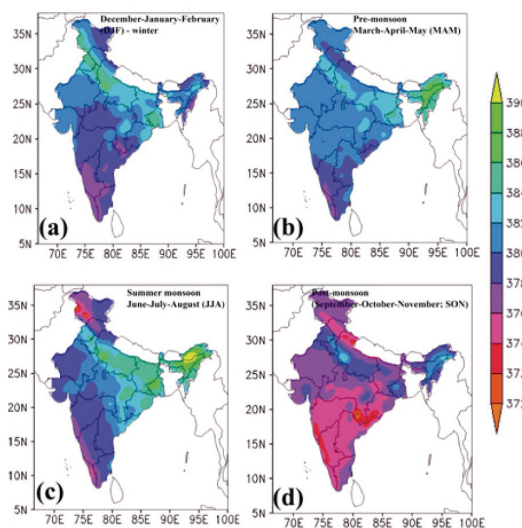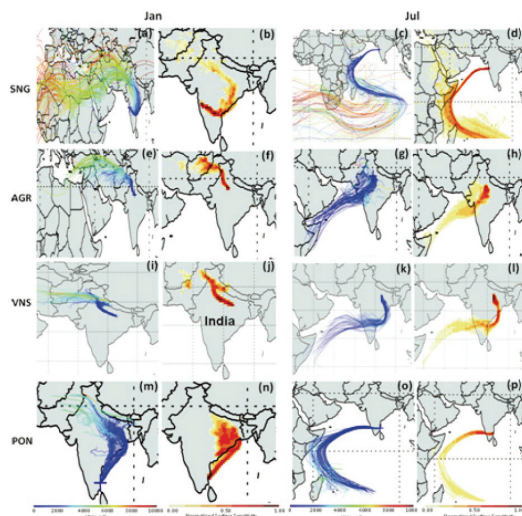
Figure 2

FLEXPART simulated air parcel back-trajectories and normalized surface emission sensitivity reaching the receptor sites(top panel a-p). The trajectories from SNG are derived backward in time for 15 days and others are for 7 days for the year 2010. (bottom panel) Mean atmospheric CO_2 mole fractions/ concentrations (ppm) during 2000-2009 valid for the (a) winter, (b) pre-monsoon, (c) monsoon, and (d) post-monsoon seasons over the Indian subcontinent from CT-Asia dataset.

Particles are transported over warmer land regions of northern hemisphere in January (Figure 2 top panel, a and b), i.e., from

western part of Asia and northern Africa, and from the oceanic regions in the southern hemisphere in July, i.e., over the cooler waters of Atlantic Ocean and southern Indian Ocean.

The Indo-Gangetic plain (IGP) region is one of the notable source regions for carbonaceous emissions due to biomass burning, coal combustion, and traffic exhaust. Upon the particle descent and entry into the Indian monsoon domain, the regional source contributions to the receptor site primarily arise from the horizontal flow in conduits within the planetary boundary layer (PBL).

The summertime conduit in July is apparently linked to the low-level cross-equatorial and southwesterly monsoonal flows (shown in blue color; Figure 2c, top panel). The winter time conduit in January (Figure 2a, top panel) is primarily due to the prevalence of subsidence over the north Indian landmass, and cold wave conditions associated with passage of extra-tropical western disturbances originating from the Mediterranean juxtaposed with the northeasterly monsoon winds from the Tibetan Plateau. The particle residence times appear to respond to the effects of large-scale monsoon circulation over a larger region of the marine atmosphere in July and to the effects of the strong continental atmospheric stability over a smaller region in January. This can be seen in the surface sensitivity maps shown in Figures 2b and 2d, top panel. These figures show the footprints of emission sensi-

tivity during January and July. Longer residence times of the particles due to upwind sources indicate stronger emission sensitivity or surface sensitivity in a given grid cell i.e., these footprints represent the sensitivity of mole fraction at the receptor site to upwind surface sources/sinks. To further understand the influence of monsoonal circulations over the Indian subcontinent on the upwind source regional sensitivities, the back-trajectory analysis is also conducted for a few other locations Agra (AGR) and Varanasi (VNS) from central India, and Pondicherry (PON) from the southern side. Unlike at SNG, the other aforementioned receptor sites showed narrow region of upwind regional sensitivity during July, while the extent of regional sensitivity increases from northern to southern sectors of the Indian subcontinent. Figure 2 (bottom panel) shows the mean CO_2 concentration for different seasons from the CT-Asia dataset. In response to stronger monsoonal flow north of the monsoon trough (ref. figure 1, left panel), one can see greater CO_2 concentrations ($\geq$ 384 ppm) widespread in the IGP region, one of the source regions for carbonaceous emissions. These elevated CO_2 events indicate a contribution of both continental and marine source regions with greater continental influences. The lower CO_2 concentration events along the west coast of India are primarily driven by marine transport mechanisms with emission source regions closer to the coastline. Upon summer monsoon withdrawal in Sep-

tember, there is a decrease in the mean CO_2 concentration values by about 6 to 8 ppm in the IGP region, and a very notable drop of about 10 ppm in the peninsular Indian region. In particular, there is a pronounced decrease (< 372 ppm) evident in the vicinity of the SNG and CRI sites across the Western Ghats region in October.
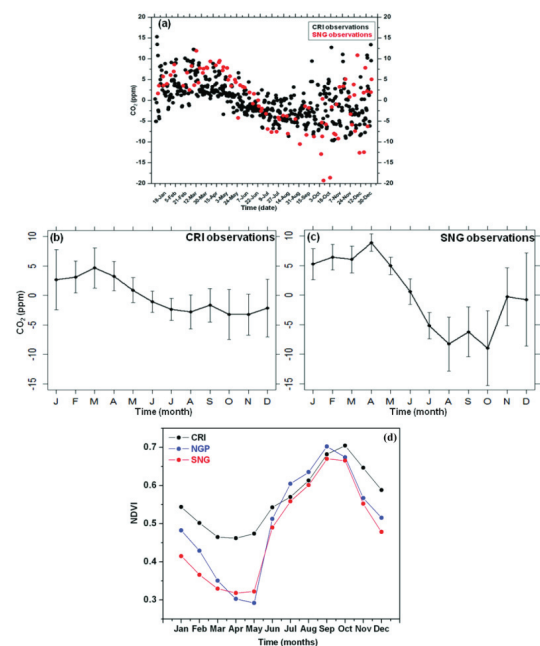

Figure 3

(a) Scatter plot of de-trended atmospheric CO_2 mole fractions (ppm) concentration valid for the observations at SNG (2010-2013) and CRI (1993-2012) and the clima-tological mean standard deviation for (b) CRI and (c) SNG. (d) NDVI climatological mean (2000-2010) at Sinhagad (SNG), Cape Rama (CRI), and Nagpur (NGP).

Prevalent dry conditions associated with higher surface pressures over the central and northern parts of India which tend to draw the extra-tropical cold and dry air streams into the IGP region, which is juxtaposed with the

advent of northeasterly winter monsoons, suggest that the continental source regions significantly impact the SNG site with sources from the IGP region.

A subjective analysis is further carried out to assess the spatial variability of CO_2 through the use of vegetation/land covers changes. Figure 3d shows the monthly climatological mean of Normalized Difference Vegetation Index (NDVI) during the period 2000-2010 at SNG, CRI as well as at Nagpur (NGP; located 800 km east from the Arabian Sea; marked by NGP in Figure 1 right panel). Irrespective of coastal and inland site locations, NDVI during the summer monsoon (JJAS) months are about the same and the corresponding NDVI values closely represent a dense green area. However, there are notable differences behind and ahead of the summer monsoon season (JJAS months) at the SNG and CRI sites－in part due to little or no precipitation or vegetation losses during this time. NDVI shows a minimum value at SNG to represent bare soil during April to May, which contrasts the maximum in October to represent the loss of vegetation canopy. Although the NDVI magnitude at CRI is larger, the month-to-month variability in the vegetation cover is found to be weaker at CRI as compared to SNG. This suggests that crop harvesting in the vicinity of SNG appears to play a role ahead of the summer monsoon season. Although the NDVI at NGP indirectly suggests similar vegetation charac-

teristics to the responses associated with the Indian monsoons, the CO_2 variability at NGP is quite contrary to the scenario seen at SNG, i.e., the variability is significant during the summer monsoon months and more pronounced during the monsoon withdrawal month in September. Figure 3a shows the de-trended atmospheric CO_2 mole fractions (concentrations) observed at SNG and CRI that are derived for the corresponding dates of observations at these sites. Figures 3b and 3c show the monthly standard deviation of these observations. One can see that there is a smaller CO_2 variability (8 to 10 ppm) during summer monsoon months (JJAS) compared to values greater than 15 ppm for the remainder of the year. This is in part due to higher vegetation cover in these months due to intermittent precipitation spells. The observational record also indicated larger variances seen at SNG during post-monsoon months (later than September) than seen at CRI. These fluctuations are likely due to the effects of crop harvesting and associated extensive biomass burning in the vicinity of the receptor sites which needs further examination with more data support.

The CO_2 spatial variability, which is apparently inclined to monsoon circulations, suggests that the seasonal prevalence of both stronger and weaker transport mechanisms over the Indian subcontinent can produce strong diversities in the source-sink mechanisms. Al-though this study provides the support

for the upwind tracer transport mechanisms to the receptor locations over the Indian subcontinent, driven by the monsoon meteorology, it is also highlights the current lack of understanding of various sink mechanisms associated with the larger temporal variability shown in the observations. This demonstrates that more spatio-temporal observations over the subcontinent is required to have a better understanding of source-sink coupled mechanisms.

References

[1] Patra, P. K., J. G. Canadell, R. A. Houghton, S. L. Piao, N.-H. Oh, P. Ciais, K. R. Manjunath, A. Chhabra, T. Wang, T. Bhattacharya, P. Bousquet, J. Hartman, A. Ito, E. Mayorga, Y. Niwa, P. A. Raymond, V. V. S. S. Sarma and R. Lasco, (2013), The carbon budget of South Asia, Biogeosciences, 10, 513-527, 2013.

[2] Rayner, P. J., R. M. Law, C. E. Allison, R. J. Francey, C. M. Trudinger, and C. Pickett-Heaps (2008), Interannual variability of the global carbon cycle (1992–2005) inferred by inversion of atmospheric CO_2 and $d13CO_2$ measurements, *Global Biogeochem. Cycles*, 22, GB3008, doi:10.1029/2007GB003068.

[3] Cherchi, A., Alessandri, A., Masina, S., Navarra, A., (2010), Effects of increased CO_2 levels on monsoons. Climate Dynamics. http://dx.doi.org/10.1007/s00382-010-0801-7.

[4] Goswami, B. N (2012) *South Asian monsoon*. In Lau WKM, Waliser DD (eds.) Intraseasonal variability in the atmosphere-ocean coupled system, Springer, Berlin, pp 21-64.

[5] Ravi Kumar K, (2014), A study of atmospheric carbon dioxide (CO_2) transport over India using monitoring and modeling techniques. *Ph.D dissertation*, University of Pune, India.

[6] Francey, R. J. et al., (2003), The CSIRO (Australia) Measurement of Greenhouse Gasses in the Global Atmosphere, Report of the Eleventh WMO/IAEA Meeting of Experts on Carbon Dioxide Concentration and Related Tracer Measurement Techniques. WMO GAW Report, 2003, 148, 97-106

[7] Stohl, A., Forster, C., Frank, A., Seibert, P., Wotawa, G., (2005) Technical note: The Lagrangian particle dispersion model FLEXPART version 6.2., Atmos. Chem. Phys., 5, 2461-2474, 2005

[8] Peters W, JB Miller, J Whitaker, AS Denning, A Hirsch, MC Krol, D Zupanski, L Bruhwiler, P. P. Tans, (2005) An ensemble data assimilation system to estimate CO_2 surface fluxes from atmospheric trace gas observations, J. Geophys. Res., 2005, 110, D24304, doi:10.1029/2005JD006157.

[9] Peters, W., Jacobson, A. R., Sweeney, C., Andrews, A. E., Conway, T. J., Masarie, K.,Miller, J. B., Bruhwiler, L. M. P., Petron, G., and Hirsch, A. I., (2007), An atmospheric perspective on North American carbon dioxide exchange: CarbonTracker, P. Natl. Acad. Sci. USA, 104, 18925−18930, 2007.

Greenhouse gases measurements in Viet Nam

Trinh Lan Phuong[1*], Duong Hoang Long[2]

Located in the tropical monsoon area, adjacent to the South China Sea and the North West Pacific Ocean, Viet Nam benefits of a temperate, mild climate. At the same time, it is also affected by numerous natural disasters, especially typhoons and floods. Since ancient times, Vietnamese people have been experienced in taking advantage of climate conditions, as well as in natural disaster prevention and preparedness. Hydro-meteorological observations and measurements under feudal dynasties have been recorded and well archived up to now. However, the hydro-meteorological activities in Viet Nam have only been systematically carried out since the late 19th century. After some interruption during WWII, observations were resumed and strengthened after the National Independence Day of Viet Nam (September 2, 1945). The main aim is serving the country's construction and defense.

In 2002, the Ministry of Natural Resources and Environment (MONRE) was established on the basis of incorporating the 7 components such as land, water, mineral and environmental resources management, meteorology and hydrology, survey and mapping. The Hydro-Meteorological Service (HMS) was officially established in 1976. The National Hydro-Meteorological Service (NHMS) - an operational unit under MONRE − is responsible for almost all functions and tasks of the former HMS.

Nowadays, developing countries like Viet Nam struggles to implement sufficiently its role while participating in the Kyoto Protocol by specific activities: building a national activities program focusing on climate change,

1. Hydro-Meteorological and Environmental Station Network Center (HYMENET), National Hydro-Meteorological Service (NHMS), MONRE
2. Science, Technology and International Cooperation Department, NHMS, MONRE

building the climate change scenarios for Viet Nam, implementing the national greenhouse gases (GHGs) inventory programs.

The monitoring of meteorological, environmental factors and greenhouse gases are located in the global climate monitoring division. The data is used for weather forecasting, disaster warning, monitoring climate change and environmental protection.

Currently, the network of automatic air quality monitoring stations in Viet Nam includes 10 stations of the NHMS of Viet Nam, 11 stations of Viet Nam Environment Administration (VEA) and provincial departments of natural resources and environment. In addition, the project: "Capacity Building and Twinning for Climate Observing Systems (CATCOS)" funded by the Swiss Agency for Development and Cooperation (SDC) and coordinated by the Federal Office of Meteorology and Climatology (MeteoSwiss) made it possible to establish greenhouse gas measurement capabilities in Viet Nam. The equipment was installed in collaboration with NHMS at Pha Din station (21.57°N, 103.52°E, 1466 m asl), a rural site in a hilly,

forested area in northern Viet Nam in February 2014. The installation allows the continuous in-situ ground-based observation of carbon dioxide, methane, carbon monoxide, water vapor and ozone next to the monitoring of optical properties of aerosols. Pha Din station was recently officially nominated for a GAW regional station by the World Meteorological Organization (WMO) since July 25, 2014.

Automatic environmental station network in Viet Nam

The network currently includes a regional atmospheric background station located at Cuc Phuong National Park.

- Measurement programme: SO_2, NO_x, CO, NH_3 are measured at 10 m height, which coincides with the wind measurement height. TSP, PM_{10}, HC, O_3 are measured at a height of about 3m.
- Frequency and monitoring mode: The frequency of monitoring complies with the guidelines of WMO and the World Health Organization (WHO) to monitor the quality of the ambient air environment.

Observed parameters	Operational Mode
Meteorology: solar radiation, ultraviolet radiation, air pressure, rainfall, wind, temperature, humidity.	Automatic monitoring equipment synchronized with the environment station
TSP, PM10	Continuous real-time values, 1 hour average, 24 hours average
SO_2, NO_x, CO, HC, O_3, NH_3	Continuous real-time values, 1 hour average, 24 hours average
Precipitation chemistry (chemical composition, pH electrical conductivity [EC])	Sampling and measurement of pH, EC over one week; The sample is then sent to a laboratory for analysis.

Table 1. List of equipment used at the Automatic Air Quality Monitoring Stations

Instrument	Model	Measurement
1. High Volume Air Sampler	120HL	Suspended particulate matter($\leftarrow 100 \mu m$) through glass fiber filter paper
2. Nitrogen Oxides Analyzer	NA-621	Chemiluminescence method
3. NH_3 Analyzer	AA-626	Using a catalyst for NH3 oxidation and NO-O_3 chemical luminescence method using NH_3 removal
4. Sulfur Dioxide Analyzer	SA-631	Ultraviolet Fluorescence method
5. Ozone Analyzer	OA-681	Ultraviolet absorption method
6. Hydrocacbon Analyzer	HA-675	Flame ionitation detection method
7. CO Analyzer	ZRF	Nondispersive infrared photometer
8. Suspended Particular Matter Monitor	SPM-312D	Reduce β-rays method
9. Acid Rain Sampler Data Process System	PID:2036	Sampling and direct measurement of pH, EC rainwater
10. Datalogger	PID:2061	Process and storage database

Automatic atmospheric monitoring stations are equipped with measuring units (see Table 1), a data logger and a transferring unit. The analysis module is connected to the data-logger, storing the data. The stations are equipped with their own power generators to ensure regular power supply to maintain the operation of the station. If a power failure occurs, the generator will kick in automatically within 30 seconds to ensure operational continuity and stability of the station. The entire 10 NHMS stations are attached to a dial up modem and transmit the data in near-real-time to the center of hydro-meteorological and environmental station network via telephone line. The datalogger in stations can be accessed remotely for controlling and trouble-shooting via telephone line.

The Pha Din Global Atmospheric monitoring station

The CATCOS-project addresses the need to improve climate observations (in the atmosphere and on glaciers) world-wide, but particularly in developing countries and countries in transition. In the atmospheric domain, the project focuses is implemented by the Paul Scherrer Institute (PSI, for the aerosol part), and by the Swiss Laboratories for Materials Testing and Research (Empa, for the atmospheric trace gas part). CATCOS aims at filling gaps on the global scale to improve the global data coverage.

The Pha Din station (see Fig. 1) is located in a region where GHG measurements are sparse. The station is located on the top of a hill. The sample inlet is at 12m above ground, which is above the canopy - this is important

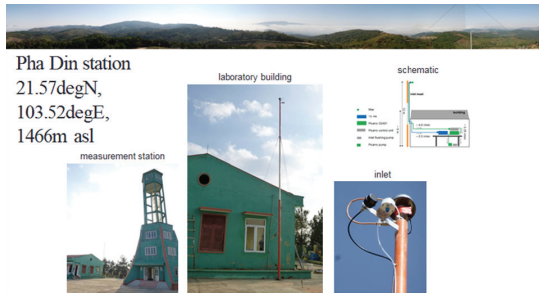for the CO_2 measurements, which would otherwise be influenced by uptake and respiration by the nearby vegetation.

Pha Din station.

The Pha Din station is the first of its kind in Viet Nam, recording greenhouse gases, surface ozone and aerosol properties in a rural setting. The GHG equipment at Pha Din station is:

- Cavity ring-down spectrometer for measuring carbon dioxide (CO_2), methane (CH_4), carbon monoxide (CO) and water vapor (H_2O) (1)
- calibration unit for spectrometer (2)
- UV absorption analyzer for measuring ozone (O_3) (3) and O_3 zero air unit (4)

- computer with data acquisition software (5)
- six cylinders with calibration gases (6)
- two pumps (7)

The first observations at Pha Din station were successfully done in March 2014 (see Fig. 2). The observations will provide important information of the impact of the strongly developing industry and biomass burning in the eastern Asian region on air quality. With the help of backward trajectories based on meteorological models (see Fig. 3), major source regions will be identified. A quantification of the emissions will then be possible.
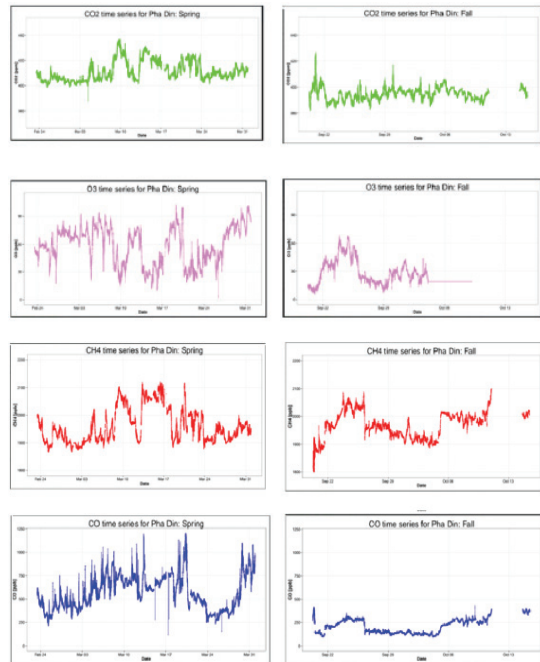
Time series of hourly averages of CO_2, O_3, CH_4, and CO in March 2014 (left) and September/October 2014 (right).
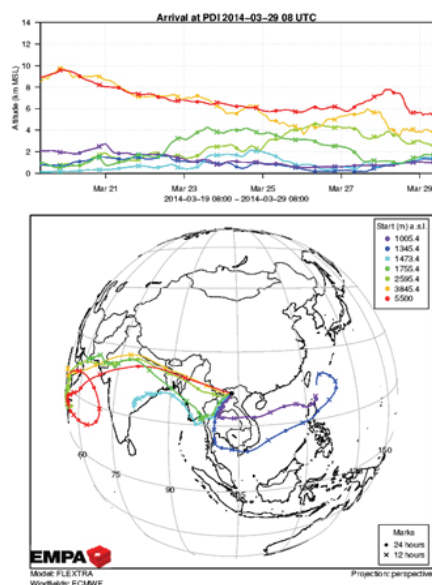
Figure 3

Backward trajectory calculation for March 29.

In Figure 2 (left panel), concentrations of the different species are shown for March 2014. Especially CO concentrations are high for a rural site with no major local emissions. The main reason for this was a high activity of forest fires on the Indochina peninsula that frequently occur during this time of the year. [5]

Figure 3 also illustrates the observed time series for September and October 2014, i.e. a season with usually only little biomass burning in this area. A comparison of the 4 different trace gases between spring (biomass burning season) and fall ("clean" season) is illustrated. Especially the CO concentrations are far higher in spring than in fall due to biomass burning. CO_2 concentrations are slightly lower in fall for the same reason. O_3 formation is also probably enhanced in spring

due to higher NO_x emissions.

Strategies and plan for the future

In the future, NHMS will:

- Expand automatic monitoring stations network.
- Improve the quantity and quality of products from automatic air quality monitoring stations data.
- Invest in human resource development, establishing training courses on the use of GHG related data in NHMS of Viet Nam.
- Maintain collaboration with WMO, other NHMSs and international cooperation.

Acknowledgements

Reference

[1] The Project CATCOS (Capacity Building and Twinning for Climate Observing System);

[2] Dr. Nicolas Bukowiecki, PSI and Dr. JÖrgKlausen, MeteoSwiss: First Viet Nam Visit of Swiss CATCOS Delegation, June 12-20, 2012;

[3] Memorandum of Understanding (MOU) between Federal Office of Meteorology and Climatology (MeteoSwiss) and National Hydro-Meteorological Service of Viet Nam (NHMS) with reference to the project CATCOS signed in May 27, 2013;

[4] Duong Hoang Long, NHMS (2013). Establishment of Continuous Greenhouse Gas Observation Capacity in Northern Viet Nam through a Swiss-Vietnamese Collaboration. Asia-Pacific GAW Greenhouse Gases Newsletter Volume No.4 December, 2013;

[5] Yen, M.-C., C.-M. Peng, T.-C. Chen, C.-S. Chen, N.-H. Lin, R.-T. Tzeng, Y.-A. Lee, C.-C. Lin, Climate and weather characteristics in association with the active fires in northern Southeast Asia and spring air pollution in Taiwan during 2010 7-SEAS/Dongsha Experiment, Atmospheric Environment, 78, 35-50.

The 6th Round robin comparison experiments and outline of the China greenhouse gas bulletin

Lingxi Zhou[1*], Pieter Tans[2], Duane Kitzis[2], Ken Masarie[2], James Butler[2], Shuangxi Fang[1], Lixin Liu[1], Bo Yao[1], Gen Zhang[1], and Siyang Cheng[1]

Brief introduction of the 6th WMO/IAEA Round Robin Comparison Experiment

The primary goal of the WMO/IAEA Round Robin Comparison Experiment is to assess the level to which participating laboratories maintain their link to the WMO mole fraction scales using normal operating procedures. Maintaining a direct link to the WMO/IAEA scales and successfully propagating the scales to working laboratory scales are fundamental to the measurement process. The primary focus of the Round Robin experiment is comparison of CO_2 scales. Many participating labs are also able to make measurements of other greenhouse gas and related tracers including CH_4, CO, H_2, N_2O, SF_6, O_2/N_2, and $\delta^{13}C$ and $\delta^{18}O$ of CO_2. Participating labs are encouraged to make these additional measurements provided the effort does not extend beyond the allotted time. Results from the periodic Round Robin experiments have proven useful to understanding the cause(s) when measurement differences between laboratories are observed. A WMO/CCL is responsible for maintaining and distributing the WMO Mole Fraction scale for a specified gas in air. NOAA/ESRL/GMD in the USA is the WMO CCL for CO_2, CH_4, N_2O, SF_6, and CO. MPI-BGC laboratory in Jena Germany is the CCL for H_2 and for the stable isotopes of CO_2. The 6th Round Robin is currently underway [started: January 2014] http://www.esrl.noaa.gov/gmd/ccgg/wmorr.

1. Chinese Academy of Meteorological Sciences, China Meteorological Administration
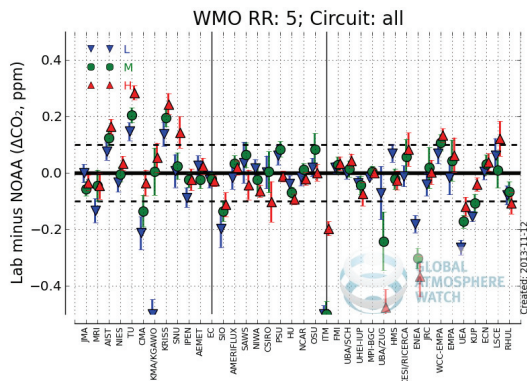2. NOAA Earth System Research Laboratory, Boulder, Colorado, USA

Figure 1

WMO/IAEA Round Robin Comparison Experiment - Archived Results (the plot shows differences for each RR cylinder measured). The dashed lines around the zero line identify the WMO recommended level of network compatibility. The measurement date and lab abbreviation did not show here on the x-label (for detail please check on the website).

Outline of the China Greenhouse Gas Bulletin

Since the 1980s, the China Meteorological Administration has put in place seven atmospheric background stations - Waliguan in Qinghai (WLG), Shangdianzi in Beijing (SDZ), Lin'an in Zhejiang (LAN), Longfengshan in Heilongjiang (LFS), Shangri-La in Yunnan (XGL), Jinsha in Hubei (JSA) and Akedala in Xinjiang (AKD), which represent a number of typical climatic, ecological and economic zones in China. GHGs and related tracers have been observed by network stations in a standard and consistent routine. In particular, the WLG GAW Global station has engaged in flask air sampling analysis since 1990 and in-situ observation since 1994, in collaboration with international colleagues.
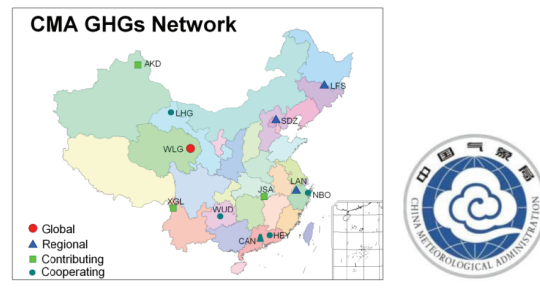

Figure 2

CMA's GHG network.

The greater than 20-year history of observations has yielded the longest time series of atmospheric CO_2 and CH_4 mixing ratio records in China. The flask air sampling analysis and the in-situ observations were launched from other background stations beginning in 2006. Echo to the WMO Greenhouse Gas Bulletin No.8 (2012), No.9 (2013) and No.10 (2014), the CMA is responsible for the China Greenhouse Gas Bulletin No.1 (2012), No.2 (2013) and No.3 (2014) based on observational datasets that are traceable to the World Reference Scales.

These scientifically defensible data sets are produced with an approach consistent with WMO guidelines and recognized QA/QC procedures (They are regularly updated and periodically revised by small amounts should the international calibration scales be adjusted).
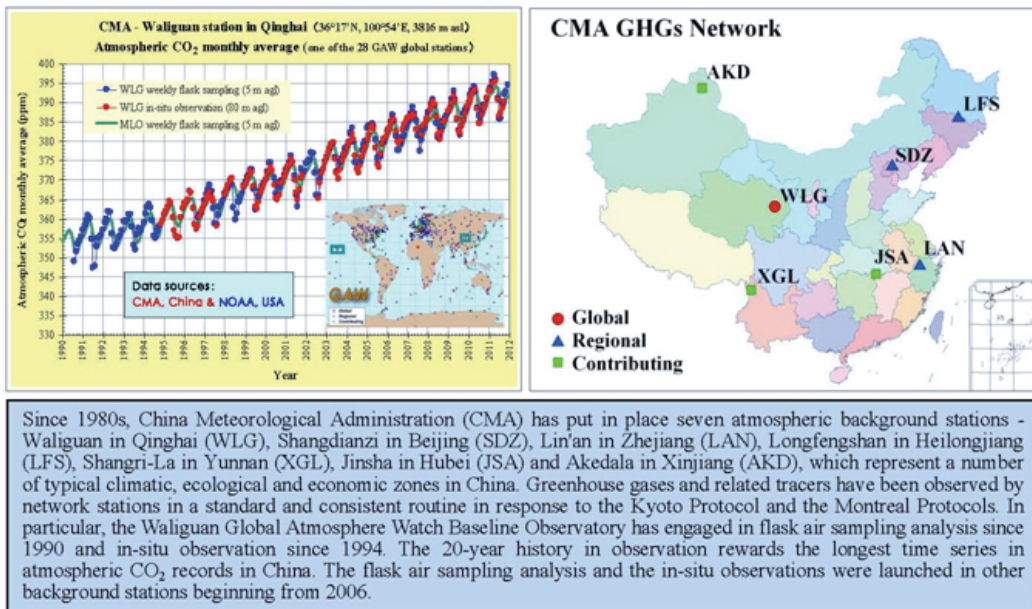
CHINA GREENHOUSE GAS BULLETIN

The State of Greenhouse Gases in the Atmosphere
Based on Chinese and Global Observations through 2011

No. 1   December 2012

Climate Change Centre
China Meteorological Administration

Since 1980s, China Meteorological Administration (CMA) has put in place seven atmospheric background stations - Waliguan in Qinghai (WLG), Shangdianzi in Beijing (SDZ), Lin'an in Zhejiang (LAN), Longfengshan in Heilongjiang (LFS), Shangri-La in Yunnan (XGL), Jinsha in Hubei (JSA) and Akedala in Xinjiang (AKD), which represent a number of typical climatic, ecological and economic zones in China. Greenhouse gases and related tracers have been observed by network stations in a standard and consistent routine in response to the Kyoto Protocol and the Montreal Protocols. In particular, the Waliguan Global Atmosphere Watch Baseline Observatory has engaged in flask air sampling analysis since 1990 and in-situ observation since 1994. The 20-year history in observation rewards the longest time series in atmospheric CO_2 records in China. The flask air sampling analysis and the in-situ observations were launched in other background stations beginning from 2006.

Executive summary

The World Meteorological Organization (WMO) Greenhouse Gas Bulletin (2011) No. 8 released by WMO on 19 November 2012 shows that globally averaged mole fractions in atmospheric carbon dioxide (CO_2), methane (CH_4) and nitrous oxide (N_2O) continued to hit new highs in 2011, with CO_2 at 390.9 ± 0.1 ppm [1], CH_4 at 1813 ± 2 ppb [2] and N_2O at 324.2 ± 0.1ppb. These values constitute 140%, 259% and 120% of pre-industrial (before 1750) levels.

As analyzed from observational data at the seven China Meteorological Administration (CMA) background stations through 2011, averaged mole fractions in atmospheric CO_2, CH_4 and N_2O also hit new highs in 2011, with the Waliguan station in Qinghai registering 392.2 ppm for CO_2, 1861 ppb for CH_4 and 324.7 ppb for N_2O. As a record high since the observation was started in 1990, they are roughly equivalent to the averaged mole fractions in the northern mid-latitudes, but are slightly higher than the global averages in all these components (390.9 ppm, 1813 ppb and 324.2 ppb) over the same period. Global mole fractions in atmospheric CO_2, CH_4 and N_2O increased by 2.0 ppm, 5 ppb and 1.0 ppb in absolute terms, from 2010 to 2011, while those at Waliguan by 2.2 ppm, 9 ppb and 1.1 ppb. Global annual averages in atmospheric CO_2, CH_4 and N_2O over the past 10 years increased by 2.0 ppm, 3.2 ppb and 0.78 ppb in absolute terms, while those at Waliguan 2.1 ppm, 3.5 ppb and 0.80 ppb.

As observed by the three regional stations of Longfengshan in Heilongjiang, Shangdianzi in Beijing and Lin'an in Zhejiang in 2011, the annually averaged mole fractions in atmospheric CO_2 were 395.8 ppm, 393.3 ppm and 400.8 ppm, those in CH_4 1942 ppb, 1887 ppb and 1942 ppb, and those in N_2O 325.5 ppb, 324.8 ppb and 326.0 ppb, all being higher than the observations made at Waliguan (392.2 ppm, 1861 ppb and 324.7 ppb) over the same period. This is somewhat a reflection of the anthropogenic impacts more active in and around the three regional background stations.

The atmospheric SF_6 mole fractions observed at Waliguan and Shangdianzi reached 7.54 ppt[3] and 7.52 ppt in 2011, - the highest ever records since the observation was launched at the two sites.

Figure 3

Atmospheric CO_2 monthly data (ppm) from Waliguan GAW global station.

The Universiti Malaya Bachok atmospheric research laboratory and 2014 NERC IOF activity: An overview

M. I. Mead[1*], A. Abu Samah[2]

Motivation

Deteriorating air quality is an increasingly acute issue in Malaysia. A rapidly increasing population and vehicle fleet coupled with industrial and agricultural activity have lead to a change in air quality. Additionally Malaysia is highly susceptible to pollution from transboundary biomass burning. The long-term potential effects of climate change are also a critical issue.

South East Asia and Malaysia in particular are relatively under characterised in terms of long term atmospheric climatologies, existing baselines as well as a rapidly changing emissions patterns. The region has a number of growing megacities (e.g. Kuala Lumpur) with increasingly pressing urban pollution issues as well as regional scale emissions footprints.

Introduction

The Universiti Malaya, Institute of Ocean and Earth Sciences, Bachok atmospheric research laboratory is part of the UM Marine Research station located in Kelantan state, Northern peninsular Malaysia. This is a new atmospheric research activity funded and operated by IOES. The station in its current form was developed by UM with significant on-going investment in infrastructure at the site both in development of the general facility as well as specifically the atmospheric research laboratory.

1. University of Manchester: School of Earth Atmospheric and Environmental Sciences (Oct 2014 - current)
   Universiti Malaya: Institute of Ocean and Earth Sciences (June 2013 - Oct 2014)
2. Universiti Malaya: Institute of Ocean and Earth Sciences

The measurement regime at the new atmospheric research laboratory was initiated in January/February 2014 coincident with the UK National Environmental Research Council International Opportunities Fund demonstration activity. This manuscript will describe the station, the prevailing conditions as well as both the IOF activity and the developing measurement capability at the station.

Station Overview

Atmospheric measurements at the Bachok site were previously undertaken in a temporary UM facility at the same location based around long-term measurements of halogenated species in partnership with the University of Cambridge (see figure 1). These were coupled with meteorological parameters as well as short-term campaign based studies for species such as O_3 and NO_x. Long-term studies started in 2008 and utilised a uDirac instrument operated in partnership between UM and UCAM with data modelling support based at UCAM (primarily using the UK Met Office NAME model).

Figure 1

The temporary research facility (left) at the Bachok site in 2010 compared with the current facility (right) in 2014 showing the huge development of the Bachok site.

The new Bachok atmospheric research facility is a tower-based laboratory located approximately 80m from the shoreline on the East coast of Peninsular Malaysia facing the South China Sea. The laboratory is located at the top of approximately 19m tall tower with sampling capability both directly to the front of the laboratory (facing the sea) as well as a collapsible mast located on the roof (see figure 2). The laboratory is ideally suited for both transport studies as well as composition observational studies due to its location. This site has been shown to have the potential to provide information on local as well as regional air masses. Dependent on season and prevailing conditions there is also the clear potential to provide information on long-range transport and composition.

Figure 2

The atmospheric research laboratory tower from the main station side (left), the beach side (middle) and the collapsible sampling mast (right) (courtesy W.Sturges).

Local Conditions of Note

Studies conducted at the Bachok site showed that during the winter there is flow dominated by the Northern South East Asian monsoon with transport from Siberian high pressure

systems across the region. In the summer flow is dominated by the South Western South East Asian monsoon with potential transport from the South e.g. from Australia (see figure 3). During transition periods between the monsoons there is considerable land sea recirculation especially when synoptic conditions aren't dominant and low wind speeds dominate overnight and in the early morning. Consequently it is clear that depending on season and prevailing conditions information can be collected at the Bachok station on local, regional and long-range composition and transport.
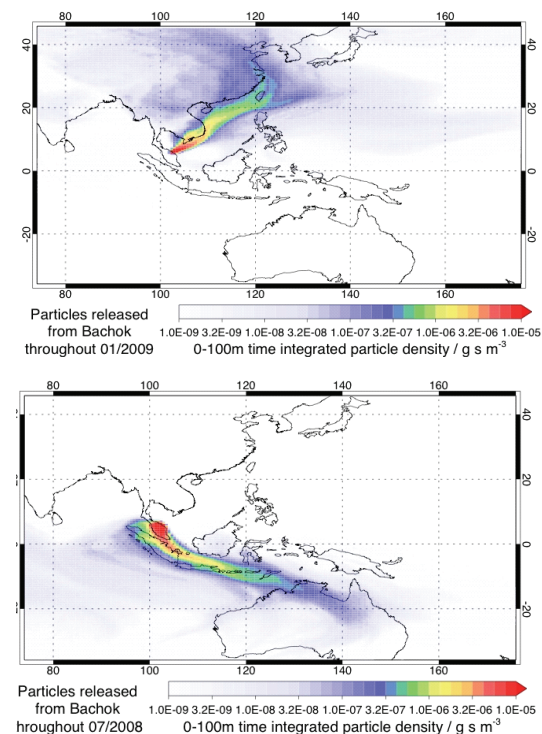
Figure 3

NAME 12 day back trajectories for the lowest 100m from Bachok. January 2009 (left) and July 2008 (right) (courtesy N. Harris).

IOF demonstration activity

The NERC IOF demonstration activity incorporated a three-week period of intensive observational measurements, collaborative instrument development as well as joint calibration studies at Bachok. For this study partners from the UK (based around a core group of NCAS partners), Australia, New Zealand and Malaysia conducted a coordinated study based at the Bachok atmospheric research laboratory.

The demonstration activity was undertaken in January and February 2014 and was a targeted intensive observational and demonstration activity lead by UCAM, UEA and UM. The activity brought over an extensive suite of instrumentation to the station to run alongside the stations own measurement capability to both demonstrate the observational utility and capability of the site as well as help create and maintain international level scientific networks. The IOF campaign activity was conducted in the late winter monsoon period during the transition out of this system. Conditions were exceptionally dry with both strong onshore winds as well as periods of slack winds (primarily in the morning).

A broad range of species was measured during this period utilising both the station's own instrumentation and a wide range of instruments from partner institutes (see table 1). A key component of the IOF activity was training and knowledge exchange between partners. This exercise also helped further

Table 1. Selected instruments deployed during the demonstration activity at Bachok

Instruments	Institute	Primary Species
uDirac	UCAM/UM	Halogenated Species
Photometer	UM	O_3
Automatic Weather Station	MMD	Local WMO Station Parameters
Cavity Enhanced Absorption Spectrometer	RHUL	$CO_2/CH_4/H_2O$
Radiosondes	UM/MMD	Temp/Humidity
Reduction Gas Analyser	UEA/YORK	CO/H_2
Pulsed Fluorescence Instruments	UEA	SO_2
	UM	
Chemiluminescence Instruments	UEA	$NO/NO_2/NO_x$
	UM	
Fluorimeter	UEA	HCHO
Proton Transfer Reaction–Mass Spectrometer (PTR-MS)	UEA	VOCs/OVOCs
Low Volume Filter	York	Aerosol Composition
Spectral radiometer	Leeds	$J(O_3)/J(NO_2)$
Aerosol analyser	UKM	Particulate Matter
Aerosol analyser	UM	
Multi Axis Differential Optical Absorption Spectroscope (MAX-DOAS)	NIWA	NO_2/Brominated Species
Whole Air Sampler	CSIRO	CO_2, $\delta13CO_2$, CH_4, H_2, N_2O
Rain Water Sampler	MMD	Acidity/Ion Content

develop international collaborative studies as well as help to further build capacity at the Bachok station. A follow up workshop was held in September 2014 at UCAM and a number of joint publications are in the process of being written based on the successful conclusion of this demonstration activity.

Developing Long-Term Capability

A number of instruments were deployed over the IOF activity period (see table 2). These primarily UM operated instruments were selected to provide long-term high quality data under a number of scientific themes in part defined by the WMO GAW programme. Specifically the "reactive trace gases", "greenhouse gases" and "aerosol" themes. There is significant cross thematic measurement potential with some of the measured metrics of importance across a number of focus areas both with WMO GAW as well as local and regional areas of scientific and regulatory interest.

The station has added to in-country observational capability for the investigation of local and trans-boundary composition as well as moving towards provision of a high quality long term baseline for climate and air quality species. One of the ultimate aims of UM relating to the Bachok atmospheric research laboratory is to become a contributing partner to the GAW regional network. It is envisaged

Table 2. Instruments currently at Bachok for long-term observational studies

Instruments	Institute	Primary Species
uDirac	UCAM/UM	Halogenated Species
Automatic Weather Station	UM	Local WMO Parameters
Cavity Enhanced Absorption Spectrometer	UM	$CO_2/CH_4/H_2O$
Reduction Gas Analyser	UEA/YORK	CO/H_2
Pulsed Fluorescence Instrument	UM	SO_2
Chemiluminescence Instrument	UM	$NO/NO_2/NO_x$
Aerosol analyser	UM	Particulate Matter
Gas Filter Correlation Analyser	UM	N_2O
Photometer	UM	O_3
Paperless Logger	UM	Integrated Data Logging

that the initial theme will be "greenhouse gases" but both "reactive gases" and "aerosol" themes have the potential for future development towards the GAW quality control requirements.

Conclusions

The UM IOES atmospheric research laboratory is a new observational tower facility located in Northern peninsular Malaysia. It is ideally sited on the coast facing the South China sea for both compositional and dynamics studies. The Bachok laboratory currently has O_3, CO, NO, NO_2, SO_2, N_2O, CO_2, CH_4, H_2O, meteorological and aerosol observational capability. The station has the potential to provide high quality data cutting across a number of thematic areas for use by the local and potentially global scientific community.

The facility has had significant infrastructural investment with large national level schemes in place at IOES. There are a number on on-going partnerships in place with UK and regional collaborators. The ultimate aim is to contribute to the WMO GAW observational network and provide high quality data products for the regional and wider global community.

List of Acronyms

UM   Universiti Malaya (Malaysia)
IOES   Institute of Ocean and Earth Sciences (Malaysia)
UMAN   University of Manchester (United Kingdom)
UCAM   University of Cambridge (United Kingdom)
UEA   University of East Anglia (United Kingdom)
NIWA   National Institute of Water and Atmospheric Research (New Zealand)
CSIRO   Commonwealth Scientific and Industrial Research Organisation (Australia)
MMD   MetMalaysia (Malaysia)

NERC   National   Environmental   Research
        Council (United Kingdom)
IOF   International   Opportunities   Fund
        (United Kingdom)
NAME   Numerical   Atmospheric - dispersion
        Modelling Environment
        (United King- dom Met Office)
WMO   World Meteorological Organisation)
GAW   WMO   Global   Atmosphere   Watch
        programme)

NERC IOF Main page: https://www.ncas.
    ac.uk/index.php/en/bachok-research-station

Acknowledgements

References and Links

µDirac: an autonomous instrument for hal-
    ocarbon measurements. / Gostlow, Brian;
    Robinson, Andrew; Harris, Niel; O'Brien, L;
    Oram, David; Mills, Graham; Newton,
    Hannah; Yong, S; Pyle, John. Atmospheric
    Measurement Techniques, Vol. 3, No. 2,
    29.04.2010, p. 507-521.

WCC-SF$_6$ activities in Korea

Haeyoung Lee[1*], Heejung Yoo[1], Jeong Soon Lee[2], Jeong-Sik Lim[2], Hongwoo Choi[1], Chulkyu Lee[1] and Bok-Haeng Heo[1]

World calibration center and standard gas

In middle of the 12th century, the term standard was used as "flag or conspicuous object" to serve as a rallying point for a military force. In modern times, the meaning of standard is not far from its etymology indicating that a standard still acts as a rallying point in the measurement field. In the field of gaseous measurements, a standard gas establishes a known analytical response to a certified chemical component concentration that this enables sample responses to be converted to a concentration whose accuracy can be determined. Due to this characteristic of a standard gas, measurement communities use standard gases in data quality assurance/ quality control (QA/ QC) protocols.

Under the World Meteorological Organization (WMO) Global Atmosphere Watch (GAW) umbrella, to ensure data quality within the network, GAW has a quality assurance framework.[1] One element in the framework is the Central Calibration Laboratories (CCL) that maintains primary standards for key greenhouse gases for participants in the inter-laboratory comparisons organized by International Bureau of Weights and Measures (BIPM). In order to minimize the difference between the analytical result and the accepted concentration of a standard, it is strongly recommended that each GAW measurement station maintain a strictly hierarchical scheme of transferring the calibration of its primary standard. However, because traceability is only an unbroken chain of calibration, this alone cannot be ensure measurement quality. Another element in the QA/QC framework

1. Korea Global Atmosphere Watch Center, Korea Meteorological Administration, Republic of Korea
2. Korea Research Institute of Standards and Science, Republic of Korea

is the World Calibration Centers (WCC), which performs station audits and develops standard operating procedures and measurement guidelines to meet the compatibility goal. According to the International Vocabulary of Metrology (VIM) a compatibility is a property of a set of measurement results of a specified measurement such that the absolute value of the difference for any pair of measured values from two different measurement results is smaller than some chosen multiple of the standard measurement uncertainties of that difference.[2] In terms of compatibility, the suggested GAW compatibility goal is 0.02 ppt for SF_6 and was expanded to 0.05 ppt in 2013.[3]

KMA (Korea Meteorological Administration) began operating a WCC for SF_6 in 2012 to support GAW stations capability to collect reliable data. Recently the WCC-SF_6 published a guideline, titled "Guideline for the analysis of SF_6 at ambient level using GC-uECD." This guideline consists of technical methods such as how to make a diagnosis and to improve SF_6 monitoring systems to meet a compatibility goal using standard gases.

Traceability and compatibility of SF_6 measurement in Anmyeondo (AMY)

In 2014, WCC-SF_6 implemented simple experiments as following the published guideline to quantify the monitoring system performance for SF_6 at Amyeondo (AMY) station in Korea. Monitoring conditions at AMY are described briefly: AMY is located in western part of Korean peninsula, downwind from China and is also affected by industrial activities in Korea assuming that high concentration episodes can occur frequently. SF_6 has been measured by GC-μECD (Agilent HP7890A) since 2007, determined using a one-point calibration every 6 hours against KRISS scale through 2012 and the WMO scale from 2013

These experiment conditions can get measurement errors from a traceability of reference gases and from a calibration method to decide the atmospheric concentration.

In order to check the instrumental performance at AMY, standard gases (WMO X2006) and ambient samples are injected 3 times for each measurement according to the operating sequence, which alternates between a standard gas and sample (Table 1). The operating conditions are shown in Table 2. The standard deviation (0.018 ppt) shows that this result is within the compatibility goal indicating that the instrument has stable response to analyze SF_6.

In terms of traceability, AMY had been using a standard gas which is traceable to the KRISS scale, but it has changed to the WMO scale since 2013. Because of this scale change, there were some challenges with data continuity and an inter-comparison experiment was designed to compare the KRISS and WMO scales. The analytical conditions are

Table 1. Measurement results from the SF$_6$ monitoring system

Sample number *	Peak area	Ratio Value $S_i \cdot 2/(R_i + R_{i+1})$	Instrumental Drift [%]
R1**	473.04		
S1***	541.89	1.1454	0.03
R2	473.17		
S2	541.80	1.1439	0.20
R3	474.10		
S3	541.31	1.1427	-0.17
R4	473.29		
S4	541.72	1.1465	-0.34
R5	471.70		
S5	541.99	1.1483	0.12
R6	472.27		
Average		1.1454	
Standard deviation		0.0022 (0.19%) 0.018 ppt	

* 3 injections per measurement, ** R: WMO X2006, FB03447, 9.595 ppt, *** S: sample collected at AMY

Table 2. Instrumental operating conditions

	Specification
Detector	μECD
Detector temp.	350 ℃
Oven temp.	35℃ 75min 30℃/min 170℃ 10min
Column	Alumina-F1 80/100 12ft*1/8 inch SUS
Sample loop	10 mL
Carrier flow	P-5, 95 mL/min
Sample flow	100 mL/min

the same as previously described. The calibration curve shown uses the WMO scale with a linear method to assign the mole fraction of SF$_6$ from the KRISS standard gas (Figure 1). The residual is -0.022 ppt, a value similar to the compatibility goal of 0.02 ppt, indicating that the difference between the two scales is small (Table 3).
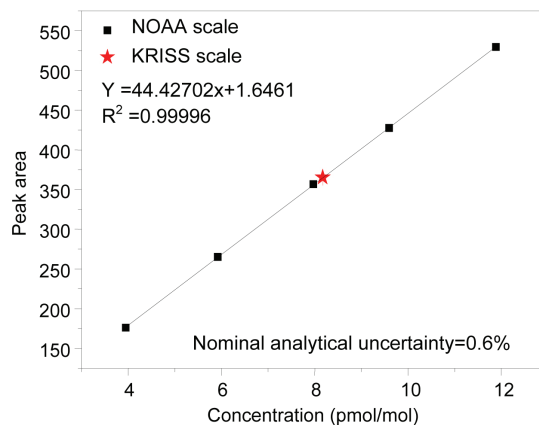
Figure 1

Calibration curve for SF$_6$ using WMO X2006 (NOAA) and KRISS scales on GC- μECD (HP 7890A).

Table 3. Comparison of SF$_6$ concentrations between WMO X2006(NOAA) and KRISS

Scale	Cylinder number	C* $_{\text{WMO X 2006}}$ [pmol/mol]	C $_{\text{calibrated}}$ [pmol/mol]	Residual	
				[pmol/mol]	[%]
WMO X2006 (NOAA)	FB03441	3.946	3.929	0.017	0.44
	FB03	5.920	5.933	-0.013	-0.22
	FB03444	7.972	7.992	-0.020	-0.25
	FB03447	9.595	9.587	0.008	0.09
	FB03450	11.887	11.879	0.008	0.07
KRISS	D068069	8.164	8.186	-0.022	-0.27

* C: Concentration

Table 4. Comparison of calibration methods   (unit : nmole/mole)

Calibration method	Multi-point (A)	Two-point (B)	One-point (C)	Difference	
				(A)–(C)	(A)–(B)
WMOX2006 (NOAA)	3.946 – 11.887*	7.972 9.595	7.972		
KRISS ** (D068069)	8.173	8.169	8.164	0.009 [0.12%]	0.005 [0.06%]

 * Refer to the range of Table 3.
** The cylinder of KRISS (D068069) was reassigned by the calibration curve against WMO2006 scale in this table.

The AMY station has used a one-point calibration method. However, it is well known that GC-ECD's response can be non-linear and that accuracy can be a concern because of error in the calibration curve. Using the WMO scale, calibration curves were made using multiple points, two points, and one point, and the KRISS standard gas was calibrated against them. When the assigned value was compared, the difference between using a multiple point and two-point calibration curve was 0.005 ppt and the difference between using a multiple point and one-point calibration curve was 0.009 ppt, with the compatibility goal (Table 4). Therefore the one-point calibration curve method is reliable only when the calibration standard concentration is similar to the target concentration.

For measurements at high and low concentrations, a multiple point calibration curve is desired. In practice, the standard gas is injected every 6 hours that the results can be used to trace the bias in the instrument.

Through this simple experiment, we could assure that the differences from different standard scale would not make the problem of the data continuity and its traceability since AMY changed reference standard gas to WMO scale in 2013. One point calibration method was reasonable to monitor background concentration, however, to meet the compatibility goal it was strongly recommended to use similar concentration of standard gases to target concentration.

Future work of the WCC-SF$_6$

According to GAWSIS, only 40 stations (17 global stations and 23 regional stations) are monitoring SF$_6$ including 20 stations with GC-ECDs and 17 stations with flask sampling method. A new guideline for less experienced laboratories who are monitoring SF$_6$ using various methods from flask sampling to continuous measurement using GC-ECD and from tube type of intake to column type GC-ECD will be published. In 2015, WCC-SF$_6$ plans to carry out an intercomparison experiment to quantify the system performance of the SF$_6$ monitoring stations and hold educational courses to improve technical performance applicable back to each station.

References

[1] WMO, Global Atmosphere Watch (2009) 15th WMO/IAEA Meeting of experts on carbon dioxide, other greenhouse gases and related tracers measurement techniques, GAW Report No, 194, pp 330.

[2] International Vocabulary of Metrology (2008) Basic and general concepts and associated terms, JCGM 200:2008, pp 90

[3] WMO, Global Atmosphere Watch (2013) 17th WMO/IAEA Meeting of experts on carbon dioxide, other greenhouse gases and related tracers measurement techniques, GAW Report No, 213, pp 168.

Various analytical techniques of SF_6 at ambient levels

Jeong Sik Lim[1], Jin Bok Lee[1], Dong Min Moon[1], A-rang Lim[1],
Hee-Jung Yoo[2], Haeyoung Lee[2], and Jeong Soon Lee[1*]

Introduction

The Global Atmosphere Watch (GAW) Program of the World Meteorological Organization (WMO) serves as an international framework aimed at maintaining the traceability chain for Greenhouse Gases observation passing through the Central Calibration Centre (CCL) and World Calibration Centre (WCC). Korea Meteorology Administration (KMA) has hosted WCC-SF_6 (World Calibration Center for SF_6) as cooperating with Korea Research Institute of Standards and Science (KRISS) and started to improve the analytical capability of SF_6.[1] In this newsletter, we present various analytical techniques for precisely measuring the concentration of SF_6 in the atmosphericfor supporting WCC task using gas chromatograph-electron capture detector (GC-ECD).

Measuring technique developments

Overview

In this letter, we will present our recent achievements on various measurement techniques of SF_6in the atmospheric. Traditionally, GC-ECD was used for analysis of SF_6 in atmospheric. Nevertheless, it's difficult to set suitable analytical condition to separate O_2 and SF_6 peaks due to strong tail of early O_2. Furthermore, since retention times of CFCs are slow, oven temperature programming ($30℃ \rightarrow 180℃$) have been performed to vent CFCs in case of real time measurement of SF_6, which might yield low degree of analytical precision. To solve the problems, we tested and compared the detailed features of two measuring techniques which are pre-concentrator coupling and fore-cutting/back-flush method. Fore-cutting/back-flush system was

1. Center for gas analysis, Korea Research Institute of Standards and Science
2. Korea Meteorological Administration

developed according to B. D. Hall *et al.* (2011).[2]

Measurement using pre-concentrator
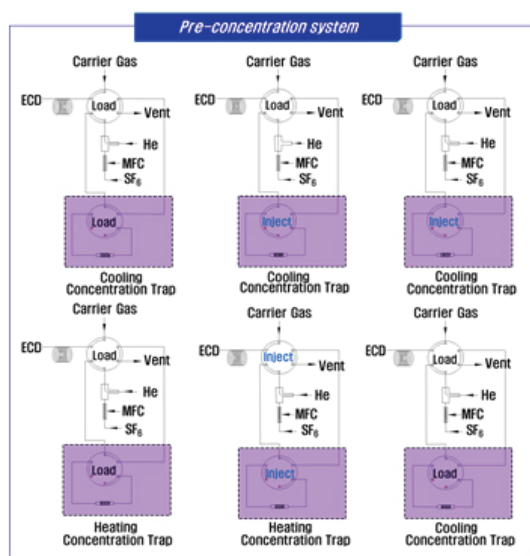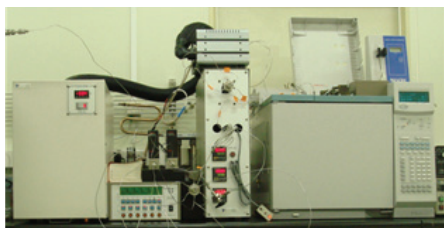
Pre-concentration system on GC-ECD. The process of concentrating gas is divided into the following six steps: 1) High-purity He is injected into the trap with the three valves turned off, and the temperature of the pre-concentrator is set at about -65℃; 2) With the pre-concentrator valve and sample injection valve turned on, the sample is adsorbed in the trap; 3) With the sample injection valve turned off, high-purity He is used to purge the non-adsorbed O_2 and the sample on the line; 4) With the pre-concentrator valve turned off, the temperature of the pre-concentrator is raised to 100°C or higher to remove the sample adhered in the trap; 5) With the other two valves turned on, the carrier gas enters the detector with the gas loaded in the trap so that SF_6, N_2O, and the CFCs can be detected; 6) During the measurement, the pre-concentrator is returned to the initial state for the next pre-concentration cycle.
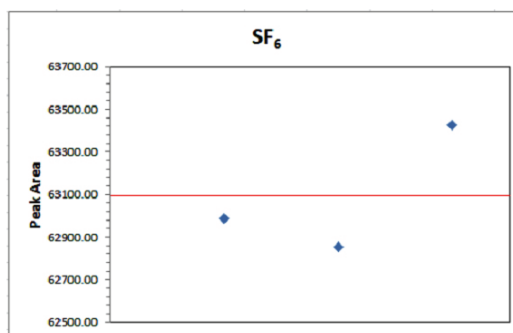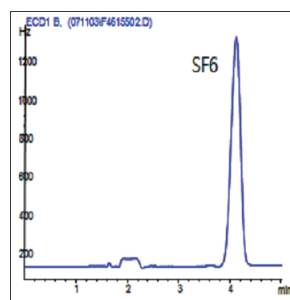
Figure 2

Chromatogram analytical repeatability of SF_6 in atmospheric. The relative standard deviation (= standard deviation/ sensitivity) is 0.048%.

A pre-concentration system was built on the basis of the GC-ECD system, as illustrated in Figure 1. In this system, samples are pre-concentrated prior to the injection. The trap where SF_6 analyteis concentrated is the core of this system. It is filled with carboxen 1000 80/100 mesh. High-purity He gas was used to purge the trap, in addition to P-5 gas that is used as a carrier gas. The pre-concentration system works in 6 phases as described in Figure caption. Figure 2 shows the chromatogram and analytical repeatability resulting from the measurement of the SF_6 in atmosphere with the GC-ECD/ pre-concentrator system, wherein only the SF_6 peak was detected. O_2, which is the under-

lying gas of the air of the reference material, was vented without being concentrated and thus its peak was not observed. This technique shows rinsing power of strong O_2 interference but total analytical precision was strongly affected by the repeatability of the pre-concentration system.
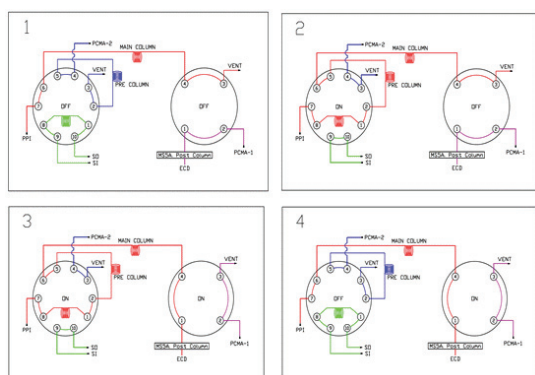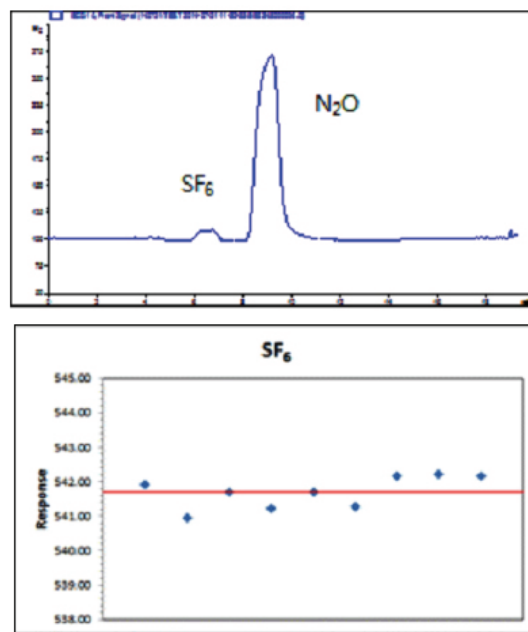
Fore-cutting/ back flush method

Figure 3

Fore cutting-back flush valve system on GC-ECD.The on-off state of the valves is configured as follows: 1) Initially, the 4-port valve is in the off-state; 2) With the 10-port valve turned on, the sample in the sample loop passes through the pre-column and main-column, and the 4-port valve is turned on so that O_2 contained in the sample can be vented; 3) After O_2 is vented, with the 4-port valve still on, SF_6, N_2O are detected; 4) If the 10-port valve is turned off, CFCs remaining in the pre-column are vented.

Figure 4

Chromatogram and analytical repeatability of SF_6 in atmospheric. The relative standard deviation (= standard deviation/ sensitivity) is 0.09%.

The fore-cutting / back-flush valve configuration, as illustrated in Figure 3, was set up as follows: instead of the conventionally used 6-port valve, 10-port and 4-port valves ware set up. This system consisted of a pre-column, main-column and post-column. Because the Molecular sieve 5A column to be used as a

Table 1. Comparison of the three analysis techniques

	GC-ECD	Pre-concentrator/GC-ECD	Fore-cutting/ back flush method
Analysis time	25 min	30 min	18 min
Interference of O_2 peak	O	X	X
Shape of SF_6 peak	Gaussian	Gaussian	Gaussian
Shape of N_2O peak	Asymmetric	-	Asymmetric
Analysis precision	0.2%	1.0%	0.2%
Remarks	Column baking required	Analysis repeatability influenced by preconcentration repeatability	

post-column required an extra temperature control, it was mounted inside the trap. Figure 4 shows the chromatogram resulting from measuring the dry air trapped in the analysis system with Alumina F1 columns mounted on it as the main column and pre-column. The first peak is the SF_6 peak, and the second corresponds to N_2O. The two peaks are clearly distinguishable. O_2 and CFCs existing in dry air were vented and thus were not detected.

Comparison among various techniques

The conventional technique for measuring the concentration of SF_6 in the atmospheric involves a simple GC-ECD analysis system. This method has been refined by monitoring a pre-concentrator to the conventional GC-ECD system. Additionally, we replaced the valve system of the conventional GC-ECD system with a new valve system that includes the fore-cutting/back flush method. These tree analysis systems are outlined in Table 1, wherein the analysis system using the fore-cutting/back flush method is shown to be the best technique in terms of analysis time, peak shape, and analysis precision.

References

[1] Lim JS *et al.* (2013). High precision analysis of SF_6 at ambient level, Atmos. Meas. Tech. 6, 2336-2342, doi:10.5194/amt-6-2293-2013.

[2] B.D.Hall *et a*l. (2011). Improving measurements of SF_6 for the study of atmospheric transport and emissions, Atmos. Meas. Tech. 4, 2441-2451, doi:10.5194/amt-4-2441-2011.

Comparison of instruments for atmospheric CO_2 observations at Baring Head, New Zealand

Sylvia Nichol, Gordon Brailsford[*], John McGregor, Peter Sperlich

Background

Measurements of atmospheric CO_2 began at Baring Head (41.4083° S, 174.8710° E) in 1972. These measurements have been made using a succession of three non-dispersive infra-red (NDIR) analysers: the URAS-1 from 1972-1977, URAS-2T from 1976-1987, and Siemens Ultramat 3 (referred to as the Siemens from now on) from 1986-present. A detailed description of the Baring Head CO_2 measurement system can be found in Brailsford et al., 2012.[1]

The Siemens is now an aging instrument, and there have been technological advances since its development. An instrument, a Picarro cavity ring down spectrometer (CRDS), which will eventually replace the Siemens has been running in parallel with the Siemens since 2011. The two instruments use the same calibration gases (8 Central Calibration La-boratory (CCL) tanks, 4 working tanks, and up to 4 "unknowns"), the same two airlines, plumbing, and cryogenic cooling, as shown in Figure 1. The same processing code is used for both instruments.

Table 1. Comparison of main features of Siemens Ultramat 3 and Picarro G2301

Siemens-Ultramat 3	Picarro–G2301
Samples at 1 Hz	Samples at ~ 0.3 Hz
64,000 bits over a range of 60ppm	"ppm" output, 4 decimal places to obtain the required sensitivity
Non-linear response	Linear response
Larger cells ~ 100 ml	Small cell size
Single pass cell	Long path length (20km)
Sensitive to water	Measures water and is sensitive to it
Coarse temperature control	Fine temperature control
Only "sees" $^{12}CO_2$	Only "sees" $^{12}CO_2$

The Picarro CRDS has some advantages over the Siemens: it measures over a wider concentration range, uses less gas, is more stable, is more linear, and also measures CH_4 and H_2O. The main features of the two instruments are summarised in Table 1. This paper compares CO_2 measurements made at Baring Head with the Siemens and the Picarro.

Instrument Response

The response of the Siemens and Picarro instruments was compared by calculating power spectra of 1-day time series of CO_2 for atmospheric air pumped from an airline, and also for air from a test tank. Air pumped directly from the atmosphere will have real variations in CO_2, and will thus test the ability of the instruments to reproduce these variations. The raw (i.e. not calibrated) atmospheric CO_2 air values were used in the analysis, as it is the raw response of the instruments that we wish to investigate. In contrast, air from the test tank will have minimal CO_2 variability and will reveal any instrumental effects on the measurements. A non-uniform sampling spectral analysis technique (Lomb-Welch periodogram[2]) was used because the Picarro samples at irregular time intervals (mean: 3 s, σ: 0.4 s), and there are also gaps in the air CO_2 time series for both instruments due to calibration runs.

The airline spectra (Figure 2a) show excellent agreement between the instruments for frequencies up to $7x10^{-3}$ Hz (corresponding to periods greater than ~140 s). Above $7x10^{-3}$ Hz the response of the Siemens falls off more rapidly than the Picarro. In the range 0.02 − 0.1 Hz a "comb filter" effect (series of peaks and troughs) is evident in the Siemens spectrum, but is not present in the spectrum from the Picarro, suggesting an instrumental effect peculiar to the Siemens.

Power spectral densities for the test tank run (Figure 2b) are several orders of magnitude lower than those for the airline data, reflecting the fact that there is minimal innate variability in the test tank air CO_2. However for frequencies up to 10^{-3} Hz (periods longer than 1000 s), the Siemens spectrum is higher than the Picarro, indicative of higher drift of the Siemens over these time scales. The fall-off in response of the Siemens is evident above 0.04 Hz (periods shorter than 25 s).

It is notable that the "comb filter" effect in

the Siemens airline spectrum is not present in the test tank data. The test tank was plumbed directly into the common inlet of the Siemens and Picarro instruments, omitting the pumping and drying stages shown in Figure 1, as the air had been dried during the process of filling the test tank. This suggests that the Siemens is sensitive to pressure or temperature fluctuations occurring in these stages. In contrast the Picarro, with its accurate control of CRDS cavity temperature and pressure, is insensitive to these influences.
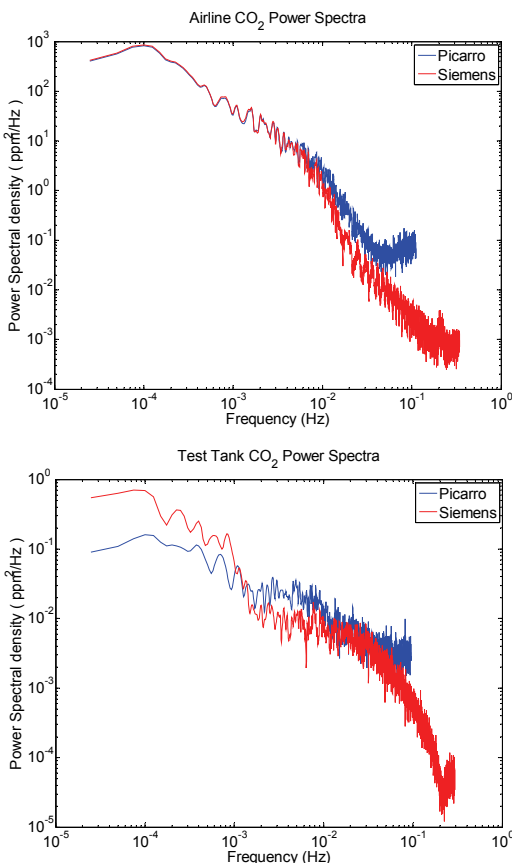
Figure 2

Power spectra for Siemens and Picarro for (a) airline CO_2 data (top panel) and (b) the test tank run (bottom panel).

CCL Tank Comparison
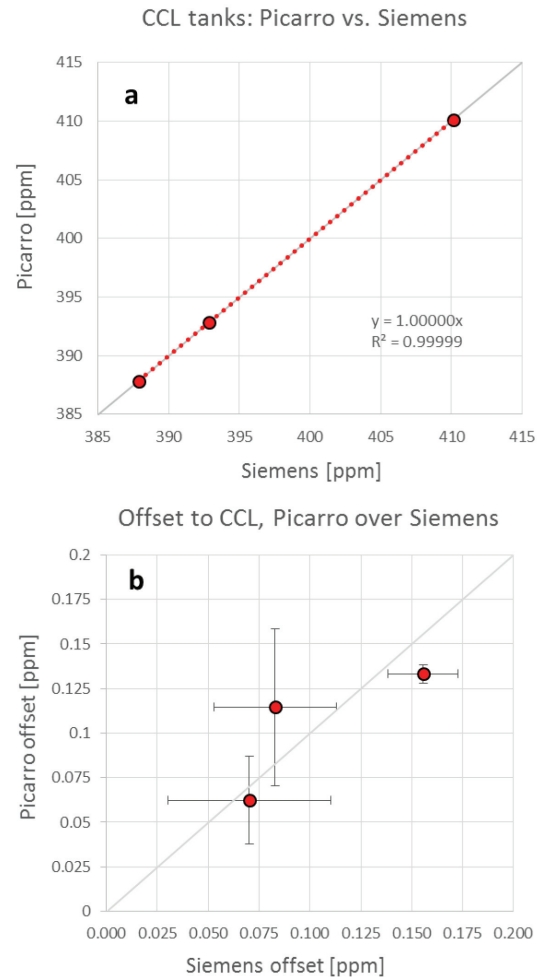
Figure 3

(a) Measured CO_2 values from the Siemens and Picarro for the three most frequently used CCL tanks; (b) Differences between the measured values for the three most frequently used CCL tanks and the CCL assigned value.

Eight calibration gases, with CO_2 mole fractions determined by the WMO CCL, are used in the measuring system as long-term transfer standards to provide a link to the WMO mole fraction scale. Figure 3a shows the measured values from the Siemens and Picarro for the

three most frequently used CCL tanks; the values in Figure 3 are the average values for measurements made in 2014 when the same reference tank was used for both instruments. Figure 3a shows very good agreement between the two instruments. Figure 3b shows, for the three CCL tanks in Figure 3a, the offset between the Siemens and Picarro measured values for these tanks (when measured as unknowns) and the CCL assigned value for each tank. The offsets for the three tanks range from 0.06 ppm to 0.16 ppm, and so are greater than the GAW compatibility goal of 0.05 ppm for southern hemisphere stations.

Isotope Effects

The CCL calibration gases are prepared with isotopic composition similar to air, this is to allow for differing instrument responses to the isotopic components. If there is a high degree of variability in the isotopic composition between the CCL tanks, then that could account for some of the offsets shown in Figure 3b. This is because both optical systems (Siemens and Picarro) are sensitive to $^{12}C^{16}O^{16}O$ only and ignore any of the rare CO_2 isotopologues. [3,4] For this reason, we investigated the isotope effect across the CCL calibration tank suite. The mole fractions of the CO_2 minor isotopologues (^{13}C and ^{18}O) were calculated for each of the eight CCL tanks, based on measurements made at NIWA. These values are shown in Figure 4. The range in ^{13}C val-

ues across the eight CCL tanks is 1.5‰, and the range in ^{18}O is 7‰. By looking at the residuals for each CCL tank from the linear fit line shown in Figure 4, we find that the isotope effect is less than 0.01ppm across the CCL calibration tank suite. Therefore, this isotope effect is much smaller than the offsets between the Siemens and Picarro CCL tank measured and assigned values (shown in Figure 3, and also included in Figure 4 for easy comparison). We estimate that a variation exceeding 10 ‰ ^{13}C or 30 ‰ in ^{18}O across the CCL tanks could produce an inconsistency between our measurements and the assigned CCL values that exceeds the GAW 0.05 ppm compatibility goal, respectively. The contribution of the isotope effect to the total disagreement in our CCL tank measurements is thus of minor importance.
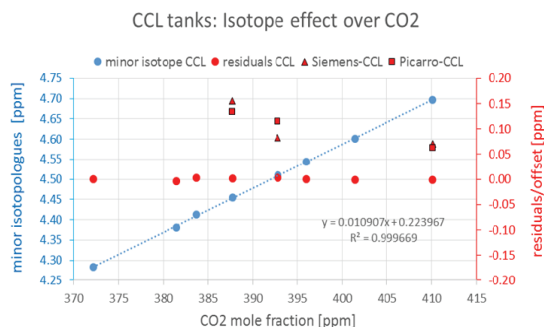

Figure 4

CO_2 minor isotopologue mole fractions versus CO_2 mole fraction for the 8 CCL tanks (blue circles, with blue linear fit line). The residuals from the linear fit line for each CCL tank are shown in red circles. The offset between the Siemens and Picarro measured values for the three most frequently used CCL tanks and the CCL assigned value (from Figure 3) are shown in red triangles and squares for comparison.
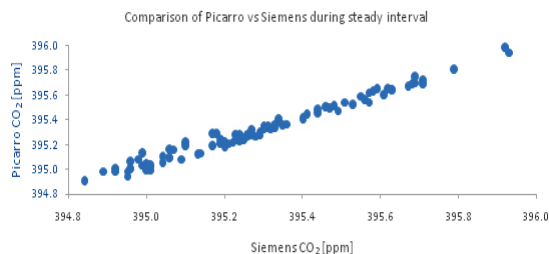
Steady interval air comparison

Figure 5

Comparison of 5-minute Siemens and Picarro CO_2 measurements of air for the steady interval on 5-6 July 2014.

The final processed air values for the Siemens are calculated using a non-linear processing routine (described in Brailsford et al, 2012[1]), and a linear regression processing routine is used for the Picarro. The processing routine utilises major calibrations, using CCL gases, to assign mole fractions to the working tanks, and then regular minor calibrations of the working tanks allow for the short term instrument variations.

During steady interval events the air arriving at the station has very low CO_2 variability, making these events a good time to compare the final processed air values from each instrument. The final processed air values show a high degree of agreement between the two instrument types (Figure 5): the mean difference between the calculated air values for each instrument is 0.03 ppm, and the standard deviation of these differences is 0.03 ppm.

While further work is required to determine why these differences exist, they are currently small and demonstrate that both instruments are currently measuring the same air in good agreement.

References

[1] Brailsford GW *et al.* (2012). Long-term continuous atmospheric CO_2 measurements at Baring Head, New Zealand, *Atmos. Meas. Tech., 5, 3109-3117*, doi: 10.5194/amt-5-3109-2012

[2] Thong, T *et al.* (2004). Lomb-Welch Periodogram for Non-uniform Sampling, *Proceedings of the 26th Annual International Conference of the IEEE EMBS San Francisco*, CA, USA, September 1-5, 2004, doi: 10.1109/ IEMBS.2004.1403144

[3] Chen H *et al.* (2010). High-accuracy continuous airborne measurements of greenhouse gases (CO_2 and CH_4) using the cavity ring-down spectroscopy (CRDS) technique, *Atmos. Meas. Tech., 3, 375-386*, doi: 10.5194/amt-3-375-2010

[4] Lee JY *et al.* (2006). Effect of carbon isotopic variations on measured CO_2 abundances in reference gas mixtures, *J. Geophys. Res., 111, D05302*, doi: 10.1029/ 2005JD006551

A new statistical method for determining regional baseline concentrations of atmospheric trace gases

Chun Ok Jo[1], Shanlan Li[1], Mi-Kyung Park[1], Haeyoung Lee[2], Chulkyu Lee[2], Kwang-Yul Kim[3] and Sunyoung Park[1,4*]

Atmospheric CO_2 concentrations which are observed at many background monitoring stations these days often reflect significant influence of anthropogenic emissions occurring on local and/or regional scales. Determining the underlying baseline or background concentration from non-baseline data can be a difficult task, but is essential to understanding the variations and trends in atmospheric CO_2 and investigating the quantitative contribution of local/regional emissions.

We present a new statistical method based on cyclostationary empirical orthogonal function (CSEOF) analysis[1,2] for determining baseline data of atmospheric trace species, applying the method to the hourly CO_2 records ob-

tained for the period from 1999 to 2012 at the Korea GAW station located in Anmyeon-do. The CO_2 time series are first detrended via least square fitting, and then decomposed via CSEOF analysis as

$$T(t) = \sum_n B_n(t) P_n(t), \qquad (1)$$

where $B_n(t) = B_n(t+d)$ are periodic functions called cyclostationary loading vectors (CSLVs) and $P_n(t)$ are principal component (PC) time series. The period d is called the nested period in CSEOF analysis and represents the periodicity of the underlying (temporal) covariance function of the given data. Note that $B_n(t)$ represent variability with time scales

1. Kyungpook Institute of Oceanography, Kyungpook National University, Daegu, Republic of Korea
2. Korea Meteorological Administration, Anmyeon-do, Republic of Korea
3. School of Earth and Environmental Sciences, Seoul National University, Seoul, Republic of Korea
4. Department of Oceanography, Kyungpook National University, Sangju, Republic of Korea

which are an integral fraction of d, whereas $P_n(t)$ represents amplitude of $B_n(t)$ varying on much longer time scales than d. In order to extract diurnal variability of CO_2, we used $d = 24$ hours in (1). Then, the resulting PC time series exhibit variability on time scales longer than 24 hours.

Thus, the PC time series are further decomposed into seasonal-scale variability to extract the seasonal cycles and their time-variant amplitudes as in (2):

$$P_n(t) = \sum_m C_m^{(n)}(t)S_m(t),$$ (2)

where $C_m^{(n)}(t) = C_m^{(n)}(t + d')$ are again CSLVs, $S_m(t)$ are corresponding PC time series, and $d' = 365$ days is the nested period for seasonal variability. As a result of double CSEOF analysis, the entire CO_2 record can be written as

$$T(t) = \sum_n B_n(t)P_n(t) = \sum_n \sum_m B_n(t)C_m^{(n)}S_m(t),$$ (3)

where $B_n(t)$ and $C_m^{(n)}(t)$ are diurnal ($d = 24$ hours) and seasonal ($d' = 365$ days) scale variations, which repeat themselves in the record.

CO_2 background concentrations are determined by investigating the nature of each PC time series. The first mode with the nested period 24 hours shows a nearly uniform diurnal structure, explaining 66.2% of the total variability. The first PC time series exhibits a long-term structure with a fairly long auto-correlation time scale, whereas the PC time series of higher modes do not exhibit any noticeable structures or substantial auto-correlation time scales. It appears that the second and third modes reflect short temporal scale events with correlation time scales less than a day or two. The first mode addressed above with the nested period of 365 days explained 23.2% of the first diurnal component. The seasonal cycles decomposed from the diurnal variations in (3) were added to the least square fit used in (1) as a detrending function, representing preliminary reconstructed background concentrations. We conduct a further analysis on these reconstructed background concentrations with the nested period of 365 days. The PC time series corresponding to the first mode exhibit increased trend throughout the year, indicating this particular mode is associated with long-term increase fit in CO_2 concentrations. Both the loading vectors and the PC time series of the second and the third modes have mean values close to zero indicating that they do not produce any net changes in CO_2 concentrations on a seasonal scale. The first PC time series is used to detrend the original CO_2 time series in (1) replacing the least square fit. The entire processes described above are repeated until the determined long-term trend is similar within $p < 0.01$ to that from the previous set of the processes.
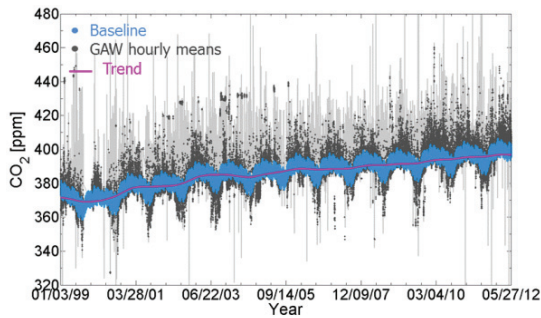
Hourly raw data of CO_2 affected by regionally polluted air masses (light gray points) at Anmyeon-do station for the 1999–2012 period, background CO_2 concentrations (light blue points) and a long-term trend (pink line) determined by a method newly proposed in this study.

Finally determined seasonal cycles of the diurnal variations in (3) plus the long-term increasing trend represent a major component of the CO_2 time series, i.e., baseline at the Korean GAW records, as shown in Figure 1. Year-to year variations in the long-term trend can be represented by time-variant modulation over a longer time span than 365 days. Unlike conventional methods for defining baseline signals (e.g., fitting the data to the sum of a second-order polynomial function and two harmonics), this method is useful for describing temporally evolving pattern of periodic components in the atmospheric trace concentrations.

A comparison was made between this newly proposed approach and a conventional method for determining the CO_2 baseline concentrations. Here, a conventional baseline solution derives from Cho et al. (2007)[3]; this particular study focuses on the long-term var-

iation of CO_2 as well as the annual cycle. The CO_2 records are fit by the following equation:

$$T(t) = c_0 + c_1 t + c_2 t^2 + \sum_{k=1}^{3} a_k \cos\omega_k t + b_k \sin\omega_k t, (5)$$

where $T(t)$ is the CO_2 record, t is time in units of days, and $\omega_k = k/365$ days are the natural frequencies. Thus, $k = 1, 2, 3$ denote respectively the annual cycle, the semi-annual cycle, and the cycle with the period of 4 months. The coefficients in (5) are determined such that the error variance in (5) is minimized. In a conventional analysis, any low-frequency components with periods greater than 50 days in the residual of fitting in (5) are added as meaningful contributions to the CO_2 background concentrations. Figure 2 shows the long-term variation of CO_2 determined according to (5) with the CO_2 baseline presented in Figure 1, which appears to describe fairly similar background structure to that based on the conventional method of parameter fitting.
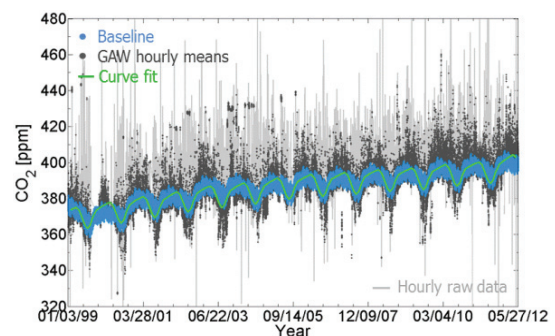
Same as Fig.1, but the curve fit in green depicts a conventional baseline determined by Cho et al., (2007).

This new method are also applied to the CO_2 time series obtained at Gosan, which is a well-known remote station located on the south-western tip of Jeju Island in Korea. In this study, data at one-hour interval from 2008 to 2012 were used. The Korean GAW center and Gosan station yield the convergent background CO_2 concentrations shown in Figure 3, suggesting that the new approach can extract basically identical regional baseline information out of the two different data sets characterized by different influences of polluted emissions. On particular, given the fact that conventional methods are applied with individual data selection criteria and low-pass filtering scheme that have been empirically determined by each regional station, this new approach seems to be more reasonable, since it is consistently applicable to different stations without using a differently pre-defined set of data selection and filtering criteria.

30-year time series data of global background CO_2 concentration from NOAA observatories at Mauna Loa are also used to examine whether the seasonal cycles and long-term trends derived by this approach are appropriate. Figure 4 demonstrates the long-term trend and variations described by the new approach are comparable to those based on the methods that NOAA has been using. There- fore, we can conclude that the new statistical method is useful at both global and region monitoring stations to identify baseline signals characterized by natural variations of CO_2 concentrations upon which local and/or regional influences act on.
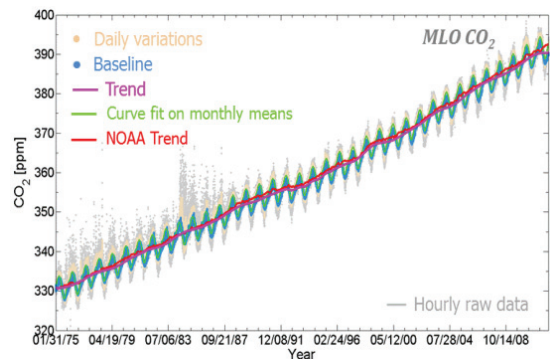

Figure 4

The new statistical approach describes diurnal variations (light peach points), the seasonal cycles (blue curve), and the long-term trend (pink line) of the CO_2 records at the MLO station for the 1975–2012 period, comparing the seasonal cycles (light green curve) and the trend (red line) based on the conventional methods that NOAA has been using.

Figure 3

Same as Fig.1, but light green data points and red curves represent the background CO_2 concentrations and the long-term trend at Gosan station for the 2008–2012 period.

References

[1] Kim, K.-Y., G. R. North, and J. Huang (1996), EOFs of one-dimensional cyclostationary timeseries: Computations, examples and stochastic modeling, *J. Atmos. Sci.*, *53*, 1007-1017.

[2] Kim, K-Y, and G. R. North (1997), EOFs of harmonizable cyclostationary processes. *J. Atmos. Sci.* 54(19): 2416-2427.

[3] Cho, C.-H., J.-S. Kim and H.-J. Yoo (2007), Atmospheric Carbon Dioxide Variations at Korea GAW Center from 1999 to 2006. *J. Kor. Meteor. Sco.* 43(4): 359-365.

Statistical data quality control using spectral analysis

Yung-Seop Lee[*] and Habin Kim

We should use adequate statistical technique through the whole process of study for estimating a good statistical model. But more important thing to proceed is statistical data quality control before the modeling. This is because un-preprocessed data may have noise and outliers which give bad effect to estimate trend or cycle of the model. We can eliminate abnormally large or small values which are produced by malfunction of the measuring instrument or typo using proper data quality control technique. Actually, there are several methods for data quality control, but this time, we introduce the method for using spectral analysis in specific type of data which has time values variable. The dataset which are used in this paper is CO_2 background concentration data provided by Korea GAW Center (Anmyeondo), from Jan 01, 2000 to Dec 31, 2013 and collected by CRDS and NDIR.

If the given dataset has time related variable, we call this time-series data. The time-series data are not independent but dependent by variable "t" which assigns time related variable. There are always 24 hours for every day, 30 days for every month and 12 months for every year. Therefore the data may have specific period like a week period or 6 months period and so on... The goal of the time-series data analysis is to find some period of the data for given dataset. In other words, if we already know the period of time-series dataset and some data points of this dataset look like against the period, then we can determine that data points are potential outliers. This is a basic concept of spectral analysis.

Most of meteorological data have 1 year cycle because of the earth's revolution. For example, the temperature of the Northern Hemisphere
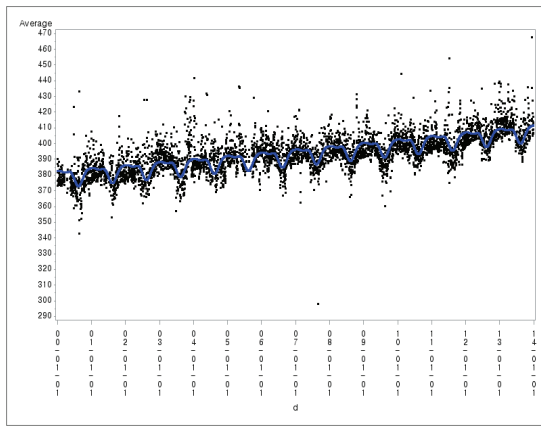
Dept. of Statistics, Dongguk University-Seoul

Figure 1

Daily CO₂ Concentration and Annual Cycle.

in January is always low and the temperature in July is always high. So we can say that the temperature of the Northern Hemisphere has 1 year cycle. This is annually repeated nature and it is meaningful to add a term which represent every 1 year cycle to the estimated model (Figure 1).

Some of meteorological phenomena didn't repeat annually since they are affected by tidal current or moon's movement. Even some phenomena could have about 200 days cycle because of some mysterious reason. In this situation, we can define such an unknown cycle of the data using **only** given dataset with the **spectral analysis.**

In spectral analysis, time-series data $X(t)$ is changed to discrete cosine transform $X_C^2(k)$ and discrete sine transform $X_S^2(k)$ for calculation of periodogram $I_X(v_k)$. Each formulation of that terms are following:

$$X_C^2(k) = \frac{1}{\sqrt{N}} \sum_{t=1}^{N} x_t \cos 2\pi v_k t$$

$$X_S^2(k) = \frac{1}{\sqrt{N}} \sum_{t=1}^{N} x_t \sin 2\pi v_k t$$

$$I_X(v_k) = X_C^2(k) + X_S^2(k), \; v_k = \frac{k}{N}; k = 1, 2, \dots, n$$

This formula means that if time-series $X(t)$ actually has frequency of v_k, then $X_C^2(k)$ and $X_S^2(k)$ cannot be 0. But if the difference between actual frequency of the time-series $X(t)$ and v_k is large, then $X_C^2(k)$ and $X_S^2(k)$ would be 0. So the large periodogram $I_X(v_k)$. means that time-series $X(t)$ has the frequency of v_k. This result is drew by calculation of regular expression of regression model.

We can find additional unknown frequency (cycle) of time-series $X(t)$ to use these method and estimate a model which can explain given data appropriately. It can be used the most powerful frequency for estimating a simplest model or can use several frequencies below some cutoff for simplifying the existing time-series model. The latter method called **low pass filtering** (Figure 2).

Through the time-series model, we can estimate the value for given time "t", and we can find the confidence interval which is a range that might have a real value. Actually, we use confidence interval for data quality control. The basic idea is to specify a cut-off value for confidence interval and to eliminate every data out of the cut-off range. Figure 3 shows
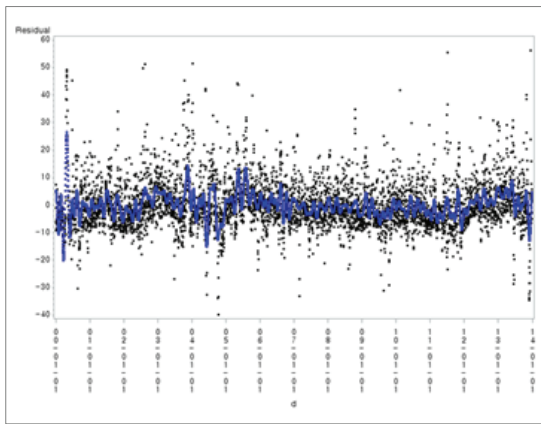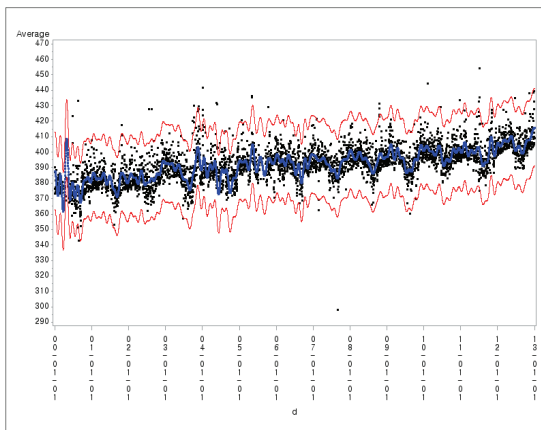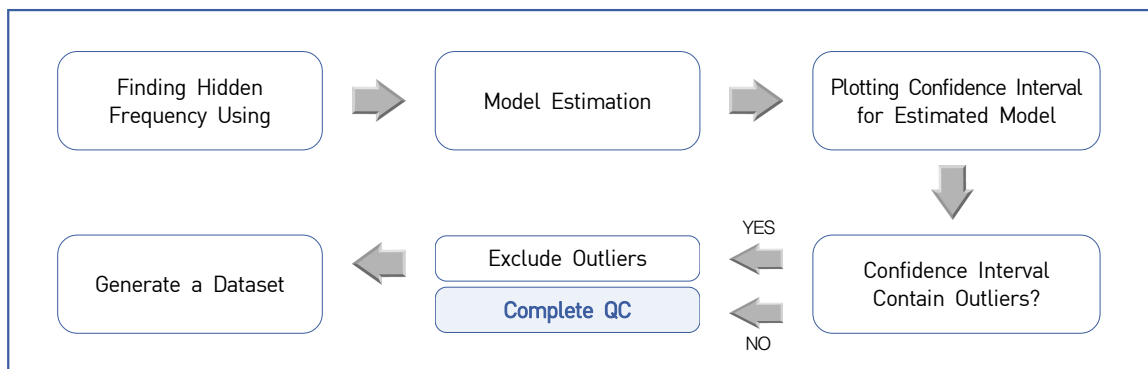
Figure 2

Low Pass Filtered Data.

Figure 3

Estimated Model and 3σ Confidence Interval.

a plot of estimated time-series model and 3σ confidence interval of this model.

There are lots of points out of the red lines. The red lines mean confidence interval. These points are regarded as outliers and should be eliminated. The process for elimination will be iterated until there are no outliers. Table 1 shows the whole process of data quality control using spectral analysis.

Figure 4 shows the iteration process using actual data. After Figure 3, there are 5 more iteration steps to get the result of the Figure 5. All points are in the range of the red lines in Figure 5. It means data QC is completed.

Table 1. Flow Chart for Data Quality Control Using Spectral Analysis
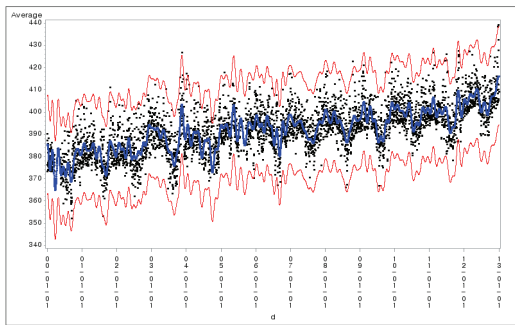
2nd Iteration
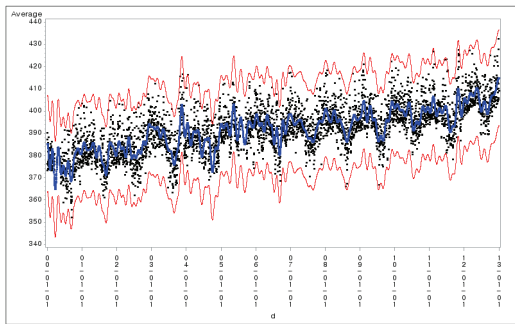
3rd Iteration
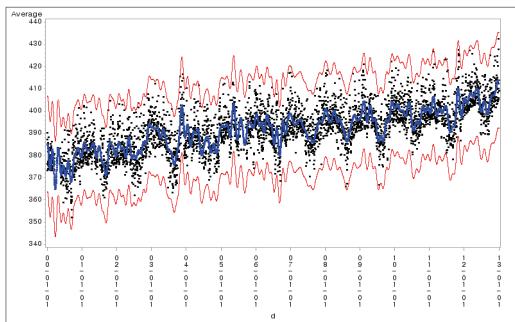
4th Iteration
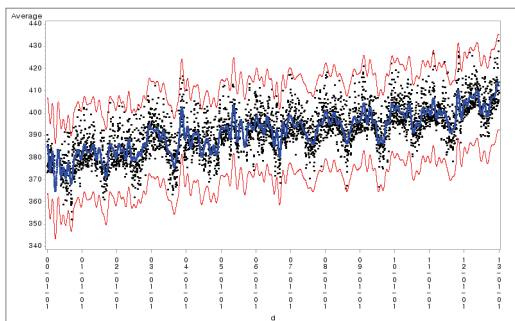
5th Iteration

Figure 4

QC Output of the each iteration.
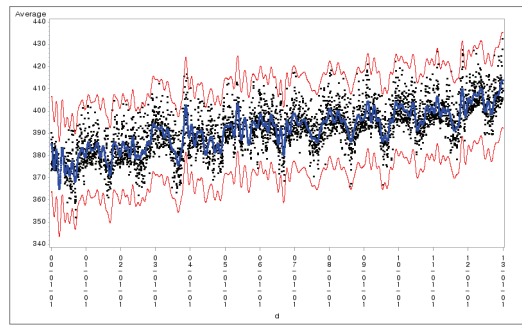
Figure 5

Quality Controlled Data.

There are variety of methods for data quality control but with this methods, we can apply not only mathematical techniques but also some information we already have had for data quality control. For example, if we know that mixing of the air in Northern Hemisphere spends 2~3 months, then it cannot have the 50 or less day's cycle for background concentration. So we can eliminate all about 50 days and less cycles using low pass filtering and this makes the analyzing output more reasonable.

We can estimate the model which is undistorted or uncontaminated using preprocessed data. Needless to say, data QC process may have the possibility of eliminating some important data. So we always think about "What makes these outliers?" and take a closer look for every data quality control steps and every outliers. This is the right attitude for good analyst.

References

[1] Conway, T. J., P. P. Tans, L. S. Waterman, K. W. Thoning, D. R. Kitzis, K. A. Masarie, and Ni Zhang, 1994: Evidence for interannual variability of the carbon cycle from the National Oceanic and Atmospheric Administration/ Climate Monitoring and Diagnostics Laboratory Global Air Sampling Network. J. Geophys. Res., 99, 22831-22855.

[2] Higuchi, K., D. Worthy, D. Chan, and A. Shashkov, 2003: Regional source/sink impact on the diurnal, seasonal and inter-annual variations in the atmospheric CO_2 at a boreal forest site in Canada, Tellus, 55B, 115-125.

[3] Inoue, H. Y., and H. Matsueda, 2001: Measurements of atmospheric CO_2 from a meteorological tower in Tsukuba, in Japan. Tellus, 53B, 2005-219.

[4] Chun-Ho Cho, Jeong-Sik Kim, and Hee-Jung Yoo, 2007: Atmospheric carbon dioxide variation at Korea GAW center from 1999 to 2006. Journal of the Korean meteorological society, 43, 4, 2007, p. 359-365.